

On the Capacity of Correlated MIMO Phase-Noise Channels: An Electro-Optic Frequency Comb Example

Mohammad Farsi, *Student Member, IEEE*, Hamdi Joudeh, *Member, IEEE*,

Gabriele Liga, *Member, IEEE*, Alex Alvarado, *Senior Member, IEEE*,

Magnus Karlsson, *Fellow, IEEE* and Erik Agrell, *Fellow, IEEE*

Abstract

The capacity of a discrete-time multiple-input-multiple-output channel with correlated phase noises is investigated. In particular, the electro-optic frequency comb system is considered, where the phase noise of each channel is a combination of two independent Wiener phase-noise sources. Capacity upper and lower bounds are derived for this channel and are compared with lower bounds obtained by numerically evaluating the achievable information rates using quadrature amplitude modulation constellations. Capacity upper and lower bounds are provided for the high signal-to-noise ratio (SNR) regime. The multiplexing gain (pre-log) is shown to be $M - 1$, where M represents the number of channels. A constant gap between the asymptotic upper and lower bounds is observed, which depends on the number of channels M . For the specific case of $M = 2$, capacity is characterized up to a term that vanishes as the SNR grows large.

Index Terms

Channel capacity, correlated phase, duality upper bound, electro-optic frequency comb, fiber optic, multiple-input-multiple-output (MIMO), phase noise channel.

M. Farsi and E. Agrell are with the Department of Electrical Engineering, Chalmers University of Technology, SE-41296 Gothenburg, Sweden (e-mail: farsim@chalmers.se; agrell@chalmers.se)

M. Karlsson is with the Department of Microtechnology and Nanoscience, Chalmers University of Technology, SE-41296 Gothenburg, Sweden (e-mail: magnus.karlsson@chalmers.se).

H. Joudeh, G. Liga, and Alex Alvarado are with the Department of Electrical Engineering, Eindhoven University of Technology (TU/e), Eindhoven, Netherlands (e-mail: h.joudeh@tue.nl, g.liga@tue.nl, a.alvarado@tue.nl).

This work was supported by the Knut and Alice Wallenberg Foundation under grant 2018.0090.

I. INTRODUCTION

Phase noise is a major issue in certain communication systems. It manifests as unwanted fluctuations in the signal phase and can severely degrade the quality and reliability of data transmission. One of the challenges in achieving higher throughputs involves the utilization of high-order constellations, which can make the entire system highly susceptible to the effects of phase noise.

To assess the effect of phase noise on the throughput of communication systems, an essential approach is to analyze the Shannon capacity. However, determining the exact capacity of a phase-noise channel, even for simple channel models, remains an open challenge. While capacity bounds and their high-signal-to-noise-ratio (SNR) approximations have been documented in the literature, a closed-form solution for the capacity of phase-noise channels is currently unavailable. The capacity of the general class of stationary phase-noise channels, including the widely used Wiener model [1], was characterized in the high-SNR regime by Lapidath [2]. Later, Katz and Shamai [3] derived upper and lower bounds on the capacity of the memoryless phase-noise channel and established that the capacity-achieving input distribution is in fact discrete.

The capacity of the single-channel Wiener phase-noise model has been extensively studied in the context of wireless and optical fiber communications (see [4]–[7] and references therein). The capacity results in [2] were extended to the multiple-input multiple-output (MIMO) phase-noise channel in [8]–[10]. The existing research covers outcomes at opposite ends of the phase-noise model spectrum. On one end, [8] characterizes the capacity of the MIMO phase-noise channel with a common phase noise using the duality approach and the “escape-to-infinity” property. On the other end, [11] derives upper bound and pre-log expressions on the capacity of MIMO phase-noise channel with separate phase noises. However, there remains an unaddressed area between [8] and [11], where correlated phase noises impact channels and multiple phase-noise sources are present. To the best of our knowledge, the capacity of such channels has never been studied in the literature.

Recently, using electro-optic frequency combs (EO-combs) as a light source in optical communication systems has led to a new variant of MIMO phase-noise channels [12], in which the phase noise is correlated across different channels. An EO-comb is a collection of equally spaced and precisely controlled optical frequencies resembling the teeth of a comb when displayed on a graph [13]. This unique property of EO-combs enables them to encode and transmit vast amounts of information simultaneously on different wavelengths. Unlike traditional approaches that rely on individual laser modules, frequency combs provide equidistant frequency tones, eliminating the need for precise wavelength control and inter-channel guard bands. Moreover, sharing a single light source results in a strong phase correlation between the comb

lines (comb lines are phase-locked to each other) which can be utilized to either increase the phase-noise tolerance [14] or decrease the complexity of the digital signal processing [15].

Recent experiments have shown that in EO-combs, the phase noises are more than 99.99% correlated between the channels [16], confirming the theoretical predictions [12] indicating the presence of two distinct phase noise terms that impact the comb. The first term arises from the continuous wave (CW) laser, which emits a constant and uninterrupted beam of coherent light, and affects all comb lines (carrier frequencies) uniformly. The second term originates from the radio-frequency (RF) oscillator and increases linearly with the number of comb lines [12]. The phase-noise model of EO-combs falls in the unaddressed area between [8] and [11] where more than one phase noise source is present and the phase noises are correlated between the channels. Intuitively, when all channels share the same source of phase noise as in [8], they can collectively enhance the achievable information rate (AIR) through joint processing. Conversely, when each channel experiences independent phase noise as explored in [11], joint processing offers no advantage. Hence, investigating capacity in scenarios where multiple channels encounter correlated phase noise from multiple sources is important as it can provide insights into optimizing joint processing techniques and their effectiveness.

A. Contributions

In this work, we investigate the capacity of a MIMO channel affected by correlated phase noises originating from the transmitter and the receiver EO-combs and additive white Gaussian noise (AWGN) from the amplifiers. In particular, the phase noise of each channel (comb line) is a combination of two independent Wiener phase-noise sources. Our contributions are as follows:

- We derive capacity upper and lower bound for MIMO channels affected by multivariate correlated Wiener phase noises originating from the transmitter and the receiver EO-combs. To derive the upper bound, we use the duality approach [17] considering a specific distribution for the output of the channel. For the lower bound, we determine a family of input distributions that results in a tight lower bound in the high-SNR regime.
- We provide high-SNR capacity upper and lower bounds that are obtained by modifying the derived upper and lower bounds. These bounds are derived through modifications to the originally derived upper and lower bounds. In particular, we show that the pre-log is one less than the number of channels. We also show that there is a constant gap between the high-SNR upper and lower bounds, where the gap is a function of the number of channels.
- We compare our bounds with lower bounds obtained by evaluating the information rates achievable with quadrature amplitude modulation (QAM) constellations numerically.

- For the 2×2 EO-comb channel, the constant gap between the high-SNR lower and upper bounds vanishes asymptotically as SNR grows large. This gives the capacity characterization in the high-SNR regime.

The remainder of the paper is organized as follows. The notation and system model are presented in Section II. The main results are provided in Section III. Numerical results and concluding remarks are given in Section V. The proofs to the theorems and lemmas within are presented in the Appendices A–D.

II. SYSTEM MODEL

A. Notation

Throughout the paper, we use the following notational conventions. All the vectors in the paper are M -dimensional and denoted by underlined letters, e.g., $\underline{x} = (x_0, \dots, x_{M-1})$ and $\underline{x}_k = (x_{k,0}, \dots, x_{k,M-1})$. The M -dimensional vector of ones is denoted by $\mathbf{1}_M = (1, 1, \dots, 1)$. Matrices are denoted by uppercase Roman letters, and the M -dimensional identity matrix is denoted by \mathbf{I}_M . Bold-face letters \mathbf{x} are used for random quantities and their corresponding nonbold counterparts x for their realizations. An N -tuple or a column vector of $(x_{m+1}, \dots, x_{m+N})$ is denoted by $\{x_i\}_{i=m+1}^{m+N}$ or $\{x_i\}_{m+1}^{m+N}$ whenever it is clear from the context; similarly, a K -tuple of vectors $(\underline{x}_{k+1}, \dots, \underline{x}_{k+K})$ is denoted by $\underline{x}_{k+1}^{k+K}$. Random processes are considered as ordered sequences and indicated inside braces, i.e., $\{\mathbf{x}_k\} = \{\mathbf{x}_k\}_1^\infty$ is a random process.

For any $a > 0$ and $d > 0$, the upper incomplete gamma function is denoted by $\Gamma(a, d) = \int_d^\infty \exp(-u)u^{a-1}du$, and $\Gamma(a) = \Gamma(a, 0)$ denotes the gamma function. The log function refers to the base-2 logarithm. The argument (phase) of a complex value is denoted by $\angle x \in [-\pi, \pi)$. The $\text{wrap}_\pi(\theta)$ function wraps θ into $[-\pi, \pi)$ and is defined as $\text{wrap}_\pi(\theta) = \text{mod}_{2\pi}(\theta + \pi) - \pi$. Moreover, $\theta \mp \phi$ and $\theta \pm \phi$ denote $\text{wrap}_\pi(\theta + \phi)$ and $\text{wrap}_\pi(\theta - \phi)$, respectively. We denote Hadamard's (component-wise) product with \circ and conjugate transpose operation with $(\cdot)^\dagger$. We use $|\cdot|$ to denote absolute value, and $\|\cdot\|$ to denote Euclidean norm. Whenever a scalar function is applied to a vector, e.g., $|x|$, $\angle x$, $\max(x)$, etc., it stands for applying the function to each element of the vector. Whenever inequalities are applied to a vector, e.g., $\underline{x} > c$, it stands for applying the inequalities to each element of the vector, i.e., $\underline{x} > c \iff x_i > c, \forall i$.

Probability density functions (pdfs) are denoted by $f_x(x)$ and conditional pdfs by $f_{y|x}(y|x)$, where the arguments or subscripts may sometimes be omitted if clear from the context. Expectation over random variables is denoted by $\mathbb{E}[\cdot]$. Sets and distributions are indicated by uppercase calligraphic letters, e.g., \mathcal{X} . The uniform distribution on the range $[a, b)$ is denoted by $\mathcal{U}[a, b)$. The Gaussian and wrapped- π Gaussian distributions with mean μ and variance σ^2 are denoted by $\mathcal{N}(\mu, \sigma^2)$ and $\mathcal{WN}(\mu, \sigma^2)$, respectively. We denote the standard zero-mean complex circularly symmetric Gaussian distribution for a scalar by

$\mathcal{CN}(0, 1)$, and for an M -dimensional vector by $\mathcal{CN}(\underline{0}, I_M)$. The von Mises (also known as Tikhonov) distribution with mean μ and scaling factor κ is denoted by $\mathcal{VM}(\mu, \kappa)$. The differential entropy rate of a stochastic process $\{\mathbf{x}_k\}$ is defined as $h(\{\mathbf{x}_k\}) = \lim_{k \rightarrow \infty} \frac{1}{k} h(\mathbf{x}_1, \dots, \mathbf{x}_k)$.

The truncated M -dimensional gamma distribution $\mathcal{G}_{\text{tr}}(\mu, \underline{\alpha}, \gamma)$ denotes the distribution of a real vector $\underline{\mathbf{r}}$ with independent elements r_m and the pdf

$$f_{\underline{\mathbf{r}}}(\underline{r}) = \prod_{m=0}^{M-1} \frac{e^{-r_m/\mu}}{\Gamma(\alpha_m, \gamma)} \mu^{-\alpha_m} r_m^{\alpha_m-1}, \quad \underline{r} > \mu\gamma \quad (1)$$

where $\mu > 0$, $\underline{\alpha} = (\alpha_0, \dots, \alpha_{M-1}) \geq 0$, $\gamma \geq 0$, and $\Gamma(\alpha_m, \gamma)$ is the upper incomplete gamma function. Note that when $\gamma = 0$, (1) is only defined for $\underline{\alpha} > 0$.

Let $\underline{\mathbf{r}} \sim \mathcal{G}_{\text{tr}}(\mu, \underline{\alpha}, \gamma)$. Then, the truncated M -dimensional distribution $\mathcal{S}\mathcal{G}_{\text{tr}}(\mu, \underline{\alpha}, \gamma)$ is the distribution of a real vector $\underline{\mathbf{s}} = \sqrt{\underline{\mathbf{r}}}$ with pdf

$$f_{\underline{\mathbf{s}}}(\underline{s}) = f_{\underline{\mathbf{r}}}(\underline{s}^2) \prod_{m=0}^{M-1} 2s_m, \quad (2)$$

where $f_{\underline{\mathbf{r}}}(\cdot)$ is defined in (1).

The truncated M -dimensional distribution $\mathcal{C}\mathcal{S}\mathcal{G}_{\text{tr}}(\mu, \underline{\alpha}, \gamma)$ with $\mu > 0$, $\underline{\alpha} \geq 0$, and $\gamma \geq 0$ denotes the distribution of a complex circularly symmetric vector $\underline{\mathbf{x}}$ whose magnitude is distributed as $|\underline{\mathbf{x}}| = \underline{\mathbf{s}} \sim \mathcal{S}\mathcal{G}_{\text{tr}}(\mu, \underline{\alpha}, \gamma)$. The pdf of $\underline{\mathbf{x}}$ is

$$\begin{aligned} f_{\underline{\mathbf{x}}}(x) &= f_{\underline{\mathbf{s}}}(|x|) \prod_{m=0}^{M-1} \frac{1}{2\pi|x_m|} \\ &= \frac{1}{\pi^M} f_{\underline{\mathbf{r}}}(|x|^2), \end{aligned} \quad (3)$$

where $f_{\underline{\mathbf{r}}}(\cdot)$ and $f_{\underline{\mathbf{s}}}(\cdot)$ are defined in (1) and (2), respectively. Note that if $\underline{\mathbf{x}} \sim \mathcal{C}\mathcal{S}\mathcal{G}_{\text{tr}}(\mu, \underline{\alpha}, \gamma)$, then $|\underline{\mathbf{x}}| \sim \mathcal{S}\mathcal{G}_{\text{tr}}(\mu, \underline{\alpha}, \gamma)$ and $|\underline{\mathbf{x}}|^2 \sim \mathcal{G}_{\text{tr}}(\mu, \underline{\alpha}, \gamma)$.

B. EO-comb Phase-Noise Channel

The EO-comb has gained popularity in experimental studies due to its simplicity in generation using standard components such as lasers, modulators, and RF sources. Furthermore, it exhibits remarkable stability and consistency over extended periods of time.

As illustrated in Fig. 1, the comb lines generated by an EO-comb can be used as carriers in a communication system by using a similar EO-comb at the receiver (but uncorrelated with the transmitter, i.e., *free-running EO-combs*) [18]. Consequently, the collective phase noise encountered in a system utilizing EO-combs is the summation of both transmitter and receiver phase noises. Typically, a comb-based optical system utilizes a large number of comb lines; thus, we are only interested in $M \geq 2$ where using EO-combs is meaningful for communication purposes.

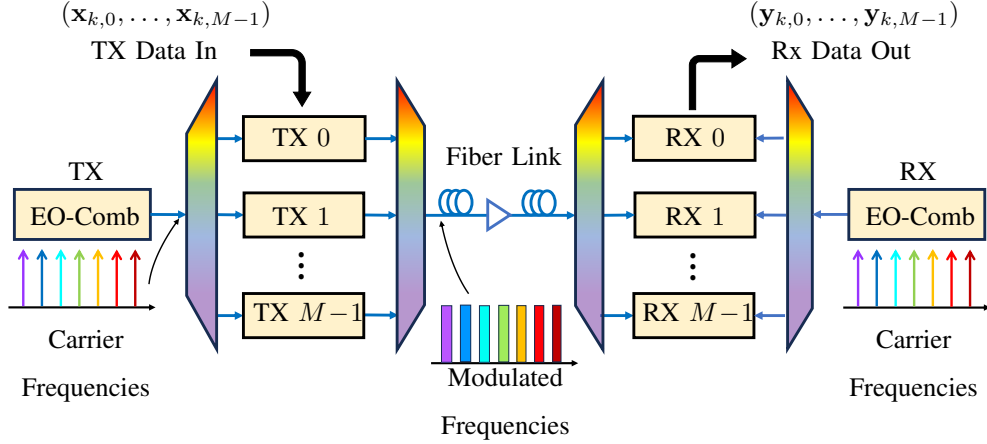


Fig. 1: The structure of a comb-based wavelength-division multiplexing (WDM) link. The transmitter and receiver (local oscillator) EO-combs are free-running (uncorrelated).

We consider a single-polarization M -dimensional MIMO transmission affected by the CW laser and RF oscillator phase noises, and amplified spontaneous emission (ASE) noise at the receiver. We also assume that nonlinearities and equalization-enhanced phase noise are negligible and chromatic dispersion is compensated.

The EO-comb channel model can be expressed as

$$\underline{\mathbf{y}}_k = e^{j\boldsymbol{\theta}_k} \circ \underline{\mathbf{x}}_k + \underline{\mathbf{w}}_k, \quad (4)$$

where $\underline{\mathbf{x}}_k = \{\mathbf{x}_{k,m}\}_{m=0}^{M-1}$ and $\underline{\mathbf{y}}_k = \{\mathbf{y}_{k,m}\}_{m=0}^{M-1}$ denote the M -dimensional input and output vectors at discrete time k , respectively. The M -dimensional vector $\boldsymbol{\theta}_k = \{\boldsymbol{\theta}_{k,m}\}_{m=0}^{M-1}$ denotes the phase-noise process. Moreover, the additive noise $\underline{\mathbf{w}}_k = \{\mathbf{w}_{k,m}\}_{m=0}^{M-1}$ is $\mathcal{CN}(\underline{\mathbf{0}}, \mathbf{I}_M)$ and independent for all k and m .

Note that the channel (4) can describe various wireless MIMO links as well as optical MIMO channels. For instance, $\boldsymbol{\theta}_k = \boldsymbol{\theta}_k \cdot \mathbf{1}_M$ with $\boldsymbol{\theta}_k$ modeled as Wiener process denotes the case of common phase noise studied in [8]. Moreover, assuming $\boldsymbol{\theta}_k = (\boldsymbol{\theta}_{k,0}, \dots, \boldsymbol{\theta}_{k,M-1})$ with independent and stationary $\boldsymbol{\theta}_{k,m}$ can describe the model studied in [11, Model B3] when only the receiver phase noise is present and the channel matrix is identity. In the following, we introduce the EO-comb phase-noise model such that two independent phase-noise sources are available and the phase noises between channels are correlated. Thus, the EO-comb phase-noise model falls in the region between [8] and [11].

The EO-comb phase noise of channel index $m \in \{0, \dots, M-1\}$ at time $k \in \{0, 1, \dots\}$ is modeled

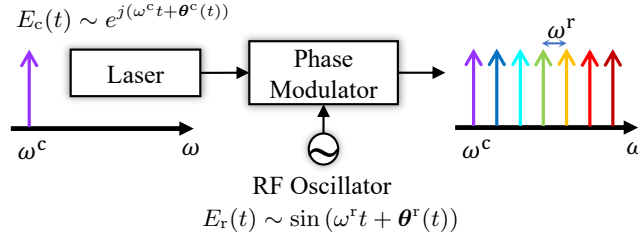


Fig. 2: A typical configuration of an EO-comb. In this setup, a CW laser at frequency ω^c with phase noise $\theta^c(t)$ is fed to a phase modulator that is driven by an RF oscillator operating at frequency ω^r with phase noise $\theta^r(t)$. This modulation process results in the generation of M comb lines characterized by a central frequency ω^c and a frequency spacing ω^r .

as¹ [12]

$$\theta_{k,m} = \theta_k^c \mp m\theta_k^r, \quad (5)$$

where θ_k^c and θ_k^r are the combined (transmitter and receiver) phase noise induced by CW lasers and RF sources, respectively. To understand where the CW laser and RF oscillator phase noises come from, we need to take the EO-comb configuration displayed in Fig. 2 into account. An EO-comb is created by employing a laser source that oscillates at the frequency ω^c with phase noise of $\theta^c(t)$. This laser is then coupled with a phase modulator that is driven by an RF source operating at frequency ω^r and phase noise of $\theta^r(t)$ [15], [19]. Note that θ_k^c and θ_k^r denote the discrete time samples of $\theta^c(t)$ and $\theta^r(t)$, respectively.

We introduce the convention c/r to prevent repeating the same equations twice. The phase-noise sources are modeled as

$$\begin{aligned} \theta_k^{c/r} &= \Delta_k^{c/r} \mp \theta_{k-1}^{c/r}, & \text{if } k = 1, 2, \dots \\ \theta_k^{c/r} &\sim \mathcal{U}[-\pi, \pi), & \text{if } k = 0, \end{aligned} \quad (6)$$

where $\Delta_k^{c/r} \sim \mathcal{WN}(0, \sigma_{c/r}^2)$ independent with $\sigma_{c/r}^2 = 2\pi B_{c/r}/R_s$. Moreover, R_s is the symbol rate and $B_{c/r} > 0$ are the CW laser and RF oscillator linewidths, respectively. Since the initial phases are $\theta_0^{c/r} \sim \mathcal{U}[-\pi, \pi)$, the processes $\{\theta_k^{c/r}\}$ and $\{\theta_{k,m}\}$ are hence stationary. The identically and independently distributed (i.i.d.) assumption on $\{\Delta_k^{c/r}\}$ implies that $\{\theta_k^{c/r}\}$ are Markov processes known as Wiener processes [8] which makes the process $\{\underline{\theta}_k\}$ a multivariate Wiener process. Note that the assumption of $\sigma_{c/r}^2 > 0$ is crucial for the validity of the results presented in this study, as it ensures that the differential entropy rate of $h(\Delta_k^{c/r}) > -\infty$.

¹Note that $\theta \mp \phi$ denotes $\text{wrap}_\pi(\theta + \phi)$ where $\text{wrap}_\pi(\theta) = \text{mod}_{2\pi}(\theta + \pi) - \pi$.

C. Channel Capacity

The capacity of the unitary MIMO phase-noise channel (4)–(6) is given by

$$C(\rho) = \lim_{n \rightarrow \infty} \frac{1}{n} \sup I(\underline{\mathbf{x}}_1^n; \underline{\mathbf{y}}_1^n), \quad (7)$$

where the supremum is over all probability distributions on $\underline{\mathbf{x}}_1^n$ that satisfy the average-power constraint

$$\sum_{k=1}^n \mathbb{E} \left[\|\underline{\mathbf{x}}_k\|^2 \right] \leq n\rho, \quad (8)$$

where ρ denotes the maximum available transmission power.

III. MAIN RESULTS

This section summarizes the main results of this work.

A. Capacity Bounds

In the following theorems, we derive upper and lower bounds on the capacity of the EO-comb phase-noise channel (4)–(6), where the phase noises are correlated across channels. Specifically, Theorems 1 and 2 characterize upper and lower bounds on the capacity $C(\rho)$ of the channel defined in (4)–(6). The proofs are located in Appendix B.

Theorem 1: For any $\lambda \geq 0$, $\underline{\alpha} = (\alpha_0, \dots, \alpha_{M-1}) > 0$, and $M \geq 2$, the capacity of the channel (4)–(6) with power constraint (8) can be upper-bounded as $C(\rho) \leq U(\rho)$, where

$$\begin{aligned} U(\rho) = & \alpha_\Sigma \log \left(\frac{\rho + M}{\alpha_\Sigma} \right) + 2 \log(2\pi) + \lambda - (M - 2) \log e + \sum_{m=0}^{M-1} \log \Gamma(\alpha_m) \\ & + \max_{\underline{s} \geq 0} \{ R_{\lambda, \underline{\alpha}}(\rho, \underline{s}) + F(M, \underline{s}, \underline{\Delta}^c, \underline{\Delta}^r) \}. \end{aligned} \quad (9)$$

Here,

$$\alpha_\Sigma = \sum_{m=0}^{M-1} \alpha_m, \quad (10)$$

$$\begin{aligned} R_{\lambda, \underline{\alpha}}(\rho, \underline{s}) = & (\alpha_\Sigma \log e - \lambda) \left(\frac{\|\underline{s}\|^2 + M}{\rho + M} \right) + \sum_{m=0}^{M-1} (1 - \alpha_m) \mathbb{E} [\log (|s_m + \mathbf{z}_m|^2)] \\ & - h(|s_0 + \mathbf{z}_0|^2 | s_0) - h(|s_1 + \mathbf{z}_1|^2 | s_1), \end{aligned} \quad (11)$$

and

$$F(M, \underline{s}, \underline{\Delta}^c, \underline{\Delta}^r) = \begin{cases} -h \left(\{ \underline{\Delta}^c \ddagger m \underline{\Delta}^r \ddagger / \underline{s}_m + \mathbf{z}_m \}_0^1 | \underline{s}, |\underline{s} + \underline{z}| \right). & M = 2 \\ -h(\underline{\Delta}^r) - h(\underline{\Delta}^c \ddagger / \|\underline{s}\| + \mathbf{v} | \underline{s}, \|\underline{s}\| + \mathbf{v}). & M > 2 \end{cases} \quad (12)$$

For future needs, $F(M, \underline{s}, \Delta^c, \Delta^r)$ is defined for a random \underline{s} , although \underline{s} is deterministic in Theorem 1. Moreover, $\Delta^c \sim \mathcal{WN}(0, \sigma_c^2)$ and $\Delta^r \sim \mathcal{WN}(0, \sigma_r^2)$ are independent; the scalar $\mathbf{v} \sim \mathcal{CN}(0, 1)$ and the elements of the vector $\underline{\mathbf{z}} = (\mathbf{z}_0, \dots, \mathbf{z}_{M-1})$ are i.i.d. and $\mathcal{CN}(0, 1)$ and independent of Δ^c , Δ^r , and \mathbf{v} .

▲

Theorem 1 is obtained by extending the method used in [8] to derive an upper bound on the capacity of the MIMO channel with a common phase noise between the channels. The proof is located in Appendix B.1.

Theorem 1 gives a family of upper bounds that can be tightened by minimizing (9) over λ and $\underline{\alpha}$. As previously mentioned, we are interested in $M \geq 2$ in this work. For the special case of $M = 1$, we refer the reader to [8, Theorem 1].

Theorem 2: For any real random vector $\underline{s} = (s_0, \dots, s_{M-1}) \geq 0$ with independent elements that satisfies the power constraint $\mathbb{E}[\|\underline{s}\|^2] \leq \rho$, the capacity of the channel (4)–(6) with power constraint (8) can be lower-bounded as $C(\rho) \geq L(\rho)$, where

$$L(\rho) = \log(2\pi) - (M-1) \log e + h(\Delta^c, \Delta^r) - 2h(\{\Delta^c \mp m \Delta^r \mp \underline{s}_m + \mathbf{z}_m\}_0^1 | \underline{s}, \{|\underline{s}_m + \mathbf{z}_m|\}_0^1) \\ + h(\underline{s}^2) - \frac{1}{2} \mathbb{E} [\log(1 + 2s_0^2)] - \frac{1}{2} \mathbb{E} [\log(1 + 2s_1^2)] - \sum_{m=2}^{M-1} \mathbb{E}[g(m, \underline{s})]. \quad (13)$$

Here, $\Delta^c \sim \mathcal{WN}(0, \sigma_c^2)$ and $\Delta^r \sim \mathcal{WN}(0, \sigma_r^2)$. The elements $\{\mathbf{z}_0, \dots, \mathbf{z}_{M-1}\}$ are i.i.d. $\mathcal{CN}(0, 1)$ and independent of all other random quantities. Moreover,

$$g(m, \underline{s}) = h(\phi(m, \underline{s}) | \underline{s}, \{s_i + \mathbf{z}_i\}_{i=0}^m) - h(\underline{s}_m + \mathbf{z}_m | s_m, |s_m + \mathbf{z}_m|), \quad (14)$$

where

$$\phi(m, \underline{s}) = \begin{cases} \underline{s}_2 + \mathbf{z}_2 \mp 2 \underline{s}_1 + \mathbf{z}_1 \mp \underline{s}_0 + \mathbf{z}_0, & m = 2. \\ \underline{s}_m + \mathbf{z}_m \mp \underline{s}_{m-1} + \mathbf{z}_{m-1} \mp \underline{s}_{m-2} + \mathbf{z}_{m-2} \mp \underline{s}_{m-3} + \mathbf{z}_{m-3}, & m > 2. \end{cases} \quad (15)$$

▲

The bound presented in Theorem 2 is a valid lower bound on the capacity for any real random vector $\underline{s} \geq 0$; hence, it can be maximized over the distribution of \underline{s} . The proof is located in Appendix B.2.

The reasoning behind selecting channel indices $m = 0$ and $m = 1$ in (11) and (13) is the requirement for two channels to acquire information about the two unknown phase noises. With the channel model exhibiting symmetry, any two adjacent channels could be chosen. For simplicity's sake, we opted for $m = 0$ and $m = 1$.

B. High-SNR Capacity Bounds

The following two theorems characterize the high-SNR behavior of the capacity of the channel (4)–(6). In the high-SNR regime, neglecting the additive noise, the output can be assumed as a rotated version of the input, i.e., $\underline{\mathbf{y}}_k \approx e^{j\theta_k} \circ \underline{\mathbf{x}}_k$; thus, we chose circularly symmetric input and output distributions to derive the high-SNR bounds. The proofs are located in Appendix C.

Theorem 3: In the high-SNR regime, the capacity of the channel (4)–(6) with power constraint (8) behaves as $C(\rho) \leq U_{\text{hsnr}}(\rho)$, where

$$U_{\text{hsnr}}(\rho) = (M-1) \log \left(\frac{\rho}{M-1} \right) + 2 \log \pi - h(\mathbf{\Delta}^c, \mathbf{\Delta}^r) + o(1), \quad \rho \rightarrow \infty. \quad (16)$$

Here, $\mathbf{\Delta}^c \sim \mathcal{WN}(0, \sigma_c^2)$ and $\mathbf{\Delta}^r \sim \mathcal{WN}(0, \sigma_r^2)$ and $o(1)$ indicates a function of ρ that vanishes in the limit $\rho \rightarrow \infty$. \blacktriangle

Theorem 3 can be interpreted as follows: at high SNRs ρ , the capacity of the M -dimensional channel (4)–(6) is upper-bounded by the capacity of an $(M-1)$ -dimensional AWGN channel plus a correction term that accounts for the memory in the channel and does not depend on the SNR ρ .

Theorem 4: In the high-SNR regime, the capacity of the channel (4)–(6) with power constraint (8) behaves as $C(\rho) \geq L_{\text{hsnr}}(\rho)$, where

$$L_{\text{hsnr}}(\rho) = (M-1) \log \left(\frac{\rho}{M-1} \right) + 2 \log \pi - h(\mathbf{\Delta}^c, \mathbf{\Delta}^r) - \sum_{m=2}^{M-1} g_{\text{hsnr}}(m) + o(1), \quad \rho \rightarrow \infty, \quad (17)$$

where $\underline{\mathbf{u}} \sim \mathcal{SG}_{\text{tr}}(1, \underline{\alpha}^*, 0)$, and

$$\alpha_m^* = \begin{cases} \frac{1}{2}, & m \in \{0, 1\}. \\ 1, & m \in \{2, \dots, M-1\}. \end{cases} \quad (18)$$

Finally,

$$g_{\text{hsnr}}(m) = \begin{cases} \mathbb{E} \left[\log \left(1 + 4 \frac{\mathbf{u}_1^2}{\mathbf{u}_0^2} + \frac{\mathbf{u}_2^2}{\mathbf{u}_0^2} \right) \right], & m = 2. \\ \mathbb{E} \left[\log \left(1 + \frac{\mathbf{u}_m^2}{\mathbf{u}_{m-1}^2} + \frac{\mathbf{u}_m^2}{\mathbf{u}_{m-2}^2} + \frac{\mathbf{u}_m^2}{\mathbf{u}_{m-3}^2} \right) \right], & m > 2. \end{cases} \quad (19)$$

The term $g_{\text{hsnr}}(m)$ in Theorem 4 is independent of the SNR ρ , and determines the gap between the high-SNR lower and upper bounds. To the best of our knowledge, there are no closed-form expressions for the expectations in (19); however, it is rather straightforward to compute them numerically.

At high SNRs, the gap between the upper and lower bounds is

$$U_{\text{hsnr}}(\rho) - L_{\text{hsnr}}(\rho) = \sum_{m=2}^{M-1} g_{\text{hsnr}}(m) + o(1), \quad \rho \rightarrow \infty, \quad (20)$$

where $g_{\text{hsnr}}(m)$ defined as in (19). For the special case of $M = 2$, we have $U_{\text{hsnr}}(\rho) - L_{\text{hsnr}}(\rho) = o(1)$ resulting in the characterization of the high-SNR capacity for $M = 2$ as

$$C(\rho) = \log \rho + 2 \log \pi - h(\mathbf{\Delta}^c, \mathbf{\Delta}^r) + o(1), \quad \rho \rightarrow \infty, \quad (21)$$

where $o(1)$ indicates a function of ρ that vanishes as $\rho \rightarrow \infty$.

From Theorems 3 and 4 it can be deduced that at high SNRs, one has to give up two real channels (one complex channel) to get full knowledge about the unknown phase noises. Thus, a feasible transmission strategy might involve utilizing the phase information from two channels (which convey no data) to estimate and then eliminate the phase noises from the remaining channels, as done in [20], [21].

IV. NUMERICAL RESULTS

In this section, we numerically evaluated the upper bound $U(\rho)$ and lower bound $L(\rho)$ in (9) and (13) and compared them with their high-SNR expressions $U_{\text{hsnr}}(\rho)$ and $L_{\text{hsnr}}(\rho)$ —the $o(1)$ terms are neglected—in (16) and (17). For every ρ , we minimized the upper bound (9) over² λ and $\underline{\alpha}$. For the evaluation of the lower bound (13), we chose $\underline{\mathbf{s}} \sim \mathcal{G}_{\text{tr}}(\mu, \underline{\alpha}, \gamma)$ where $\mu = \rho/(M - 1)$ and $\gamma > 0$. Then, we maximized the lower bound over³ γ and $\underline{\alpha}$ such that

$$\mathbb{E}[\|\underline{\mathbf{s}}\|^2] = \mu \sum_{m=0}^{M-1} \frac{\Gamma(1 + \alpha_m, \gamma)}{\Gamma(\alpha_m, \gamma)} \leq \rho, \quad (22)$$

is satisfied. We optimized parameters using the Nelder–Mead simplex algorithm [22] accompanied by the Lagrange multiplier method to handle the power constraint (22). We also employed the toolbox in [23] for the numerical evaluation of differential entropy terms in both upper and lower bounds.

We also considered the capacity

$$C_{\text{awgn}}(\rho) = M \log \left(1 + \frac{\rho}{M} \right) \quad (23)$$

of an AWGN channel with per-channel SNR equal to ρ/M , which is intuitively a good upper bound on $C(\rho)$ of the channel (4)–(6) at low SNR as the additive noise is the dominant source of impairment. The AIRs using 64-QAM and 1024-QAM, which is a lower bound on $C(\rho)$, are denoted by $L_{64\text{-QAM}}(\rho)$ and $L_{1024\text{-QAM}}(\rho)$, respectively. We evaluated these rates using the algorithm proposed in [4] for computation of the information rates for finite-state channels. Specifically, we used 512 levels for the discretization of the phase-noise process and a block of 2000 channel uses. Additionally, we visually represented a shaded region denoting the ‘‘Capacity Area’’. This area spans between the minimum value among

²Our analysis was confined to the intervals of $0 < \underline{\alpha} \leq 10$ and $0 \leq \lambda \leq 2M\alpha_{\Sigma}$, with α_{Σ} defined in (10).

³We restricted our analysis to the range of $0 < \underline{\alpha} \leq 5$ and $0 \leq \gamma \leq 2/(e^{2M/(M-2)} - 1)$.

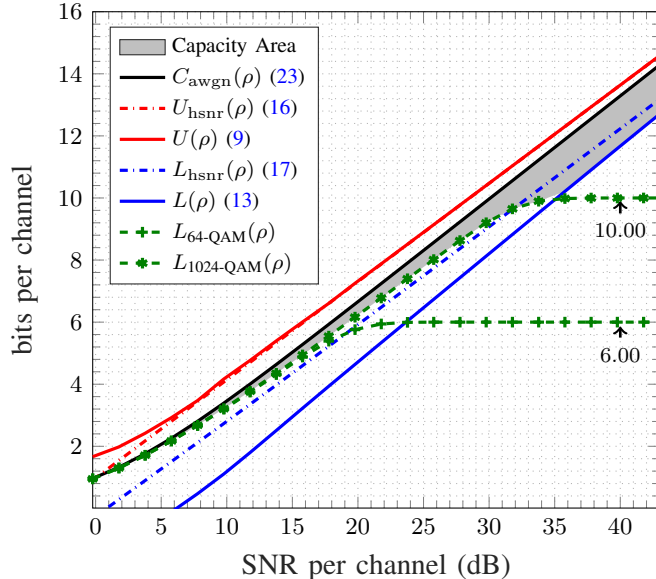


Fig. 3: Upper and lower bounds on the capacity of the channel (4)–(6) and $M = 21$, $v_c = 5 \cdot 10^{-6}$, and $v_r = 5 \cdot 10^{-9}$, i.e., $\sigma_c^2 = \pi \cdot 10^{-5}$ and $\sigma_r^2 = \pi \cdot 10^{-8}$.

all upper bounds, i.e., $\min(U(\rho), C_{\text{awgn}}(\rho))$, and the maximum value among the lower bounds, i.e., $\max(L_{64\text{-QAM}}(\rho), L_{1024\text{-QAM}}(\rho), L(\rho))$.

We define the normalized linewidth $v_{c/r} = B_{c/r}/R_s$ (linewidth divided by symbol rate). In practice, the symbol rate R_s is in the range 0.1–100 Gbaud, and the number of channels is typically high ($M > 10$) in a system utilizing EO-combs. The laser linewidth B_c and RF oscillator linewidth B_r are typically in the range of 1–1000 kHz and 1–1000 Hz, respectively. Hence, the normalized linewidth of the CW laser v_c may vary in the range of $10^{-8} - 10^{-2}$ depending on the particular application and transmission scenario. Similarly, the normalized linewidth of the RF oscillator v_r could fall within the range of $10^{-11} - 10^{-5}$.

Here, we utilized real-world channel parameters by setting⁴ $v_c = 5 \cdot 10^{-5}$ and $v_r = 5 \cdot 10^{-9}$, corresponding to $\sigma_c^2 = \pi \cdot 10^{-5}$ and $\sigma_r^2 = \pi \cdot 10^{-8}$. Fig. 3 shows the bounds for $M = 21$, where it can be seen that $C_{\text{awgn}}(\rho)$ is a tighter upper bound than our bound throughout the studied SNR range as it performs closer to the lower bound from the QAMs and $L(\rho)$. This is expected, since with the selected channel parameters, the phase noise is extremely low. As a result, the additive Gaussian noise emerges as the dominant impairment within the shown SNR range. Consequently, the capacity is expected to closely resemble that of the AWGN channel. Furthermore, the converging nature of $U(\rho)$ towards $C_{\text{awgn}}(\rho)$ curve is evident, and they are projected to intersect at higher SNR levels. However, such high SNR values fall

⁴As an example one can set the symbol rate $R_s = 20$ Gbaud, $B_c = 100$ kHz, and $B_r = 100$ Hz.

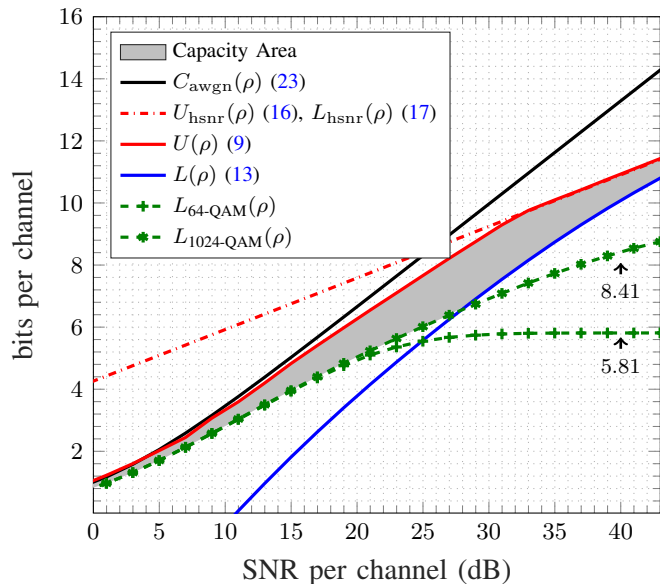


Fig. 4: Upper and lower bounds on the capacity of the channel (4)–(6) and $M = 2$, $v_c = 5 \cdot 10^{-3}$, and $v_r = 5 \cdot 10^{-5}$, i.e., $\sigma_c^2 = \pi \cdot 10^{-2}$ and $\sigma_r^2 = \pi \cdot 10^{-4}$.

beyond practical relevance. From the analysis, we can conclude that in scenarios with extremely low phase noises—typical in practical EO-comb applications—the AWGN capacity serves as a sufficiently stringent upper bound.

In Fig. 4, we show the results for $M = 2$ with $v_c = 5 \cdot 10^{-3}$, and $v_r = 5 \cdot 10^{-5}$, which correspond to $\sigma_c^2 = \pi \cdot 10^{-2}$ and $\sigma_r^2 = \pi \cdot 10^{-4}$. It can be seen that $U(\rho)$ is a tighter upper bound than $C_{\text{awgn}}(\rho)$ throughout the studied SNR range. The bound $L_{1024\text{-QAM}}(\rho)$ is tighter than $L(\rho)$ up to about 28 dB, above which $L(\rho)$ is tighter. This behavior is expected, as the input distribution for the $L(\rho)$ is chosen such that it achieves the capacity at high SNRs. The lack of saturation in $L_{1024\text{-QAM}}$ to its designated nominal point of 10 bits per channel can be attributed to the average constellation rotation induced by phase noise, which consistently surpasses the maximum tolerable rotation for the 1024-QAM constellation. The bounds approach the high-SNR expressions as the SNR increases, confirming that the high-SNR capacity for $M = 2$ follows Theorem 3. It is important to emphasize that the case where $M = 2$ lacks practical relevance in systems employing EO-combs as a light source. Nevertheless, from an information-theoretic perspective, this scenario holds significance as it serves to illustrate the capacity achieved at high SNR, as expressed in (21).

In Fig. 5, results are shown for $M = 21$. The upper bound $C_{\text{awgn}}(\rho)$ is tighter up to 28 dB (see the magnified window on the figure); then, $U(\rho)$ becomes tighter. This behavior mainly comes from the $F(\cdot)$ function defined in (12), where we used a loose upper bound for $M > 2$. The bounds approach the

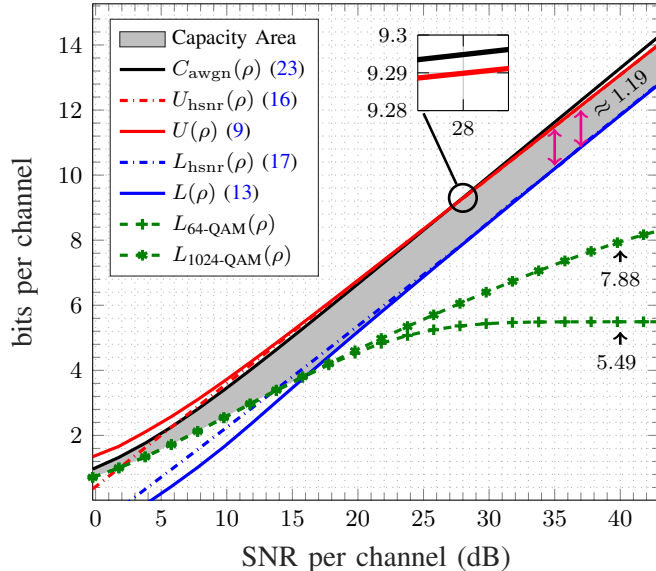


Fig. 5: Upper and lower bounds on the capacity of the channel (4)–(6) and $M = 21$, $v_c = 5 \cdot 10^{-3}$, and $v_r = 5 \cdot 10^{-5}$, i.e., $\sigma_c^2 = \pi \cdot 10^{-2}$ and $\sigma_r^2 = \pi \cdot 10^{-4}$.

high-SNR expressions as the SNR increases. Moreover, at high SNR, the gap between the lower bound $L(\rho)$ and the upper bound $U(\rho)$ approaches a constant gap (approximately 1.19 bits per channel) as expressed in (19).

While the linewidth of the studied CW laser and RF oscillator, as depicted in Figs. 4 and 5, may not currently hold practical significance, the ongoing trend in optical communication systems is geared towards developing more cost-effective and accessible solutions. This trajectory may lead to the utilization of lower-cost lasers and oscillators characterized by higher linewidths. Furthermore, in specific applications like space communications, exceptionally low symbol rates may be employed, resulting in elevated normalized linewidth values. Consequently, the mentioned figures can offer valuable insights into assessing the influence of the linewidth of the CW laser and RF oscillator on the capacity of the EO-comb channel. This is especially relevant in the context of emerging cost-conscious and accessible system designs or potential applications in specialized niches.

V. DISCUSSION AND CONCLUSIONS

We obtained lemmas that establish upper and lower bounds for the generic MIMO channel under the influence of multivariate Wiener phase noise. These lemmas can serve as a foundation for deriving capacity bounds across various phase-noise models. Then, we studied the capacity of a MIMO channel affected by correlated phase noises originating from EO-combs. Specifically, the phase noise of each channel (comb

line) is a combination of two independent Wiener phase-noise sources: the CW laser phase noise, which uniformly affects all channels, and RF oscillator phase noises that increase linearly with the channel number. We derived lower and upper bounds on channel capacity, illustrating the capacity's behavior for various values of SNR and phase-noise parameters. Additionally, high-SNR capacity upper and lower bounds were derived, revealing a pre-log of $M - 1$, where M represents the number of channels. A physical intuition to the loss of one complex channel (equivalent to two signal space degrees of freedom) is attributed to the sacrifice of two real dimensions to account for the impact of the two phase noise sources. Hence, a viable transmission scheme could be using the phase of two channels (which carry no data) to estimate the phase noises and remove them from the rest of the channels. The same intuition can be employed to justify the high-SNR capacity bound derived in [8], wherein the pre-log becomes $M - 1/2$ due to the presence of only one unknown phase noise source.

Numerical evaluations indicated that in scenarios with extremely low phase noises—typical in practical optical applications—the AWGN channel capacity serves as a sufficiently accurate upper bound.

While the capacity bounds presented in this paper are initially derived for a specific EO-comb phase-noise channel, the majority of techniques and derivations hold a general applicability that can be adapted for various phase-noise channels. More specifically:

- The capacity upper bound (69) from Lemma 16 applies not only to the EO-comb phase-noise model (5–6) but also to any phase noise modeled as a multivariate Wiener process. Hence, altering the upper bounds for a different channel requires revisiting (70) from Lemma 17, which utilizes the duality bound, and (72) from Lemma 18, which exploits the memory and correlations. Note that the techniques in the proofs of the aforementioned lemmas are general to some extent and could be reused.
- The capacity lower bound (75) in Lemma 19 is not limited to EO-comb phase-noise model (5)–(6) and remains valid even if the phase-noise vector is modeled as a multivariate Wiener process. Therefore, adjusting the lower bound for a different channel involves deriving the right-hand side (RHS) terms in (75). The choice of the input distribution and its parameters depends on the channel parameters and requires careful consideration.
- The results can also potentially be extended to account for more than two phase-noise sources. One example would be the soliton microcombs channels where phase noise arises from three different sources, namely, CW laser, pump laser, and shot noise [24]. Our hypothesis is that the pre-log term might alter to $M - d/2$ where d is the number of independent phase-noise sources. The rationale behind our hypothesis is that one needs to sacrifice d complex channels to gain the full knowledge of d unknown phases.

An interesting open question is to establish tighter upper bounds in the low-SNR regime for $M > 2$. We believe the lack of tightness in the upper bound originates from (72) in Lemma 18, where the derived bound on mutual information is loose and could potentially be refined. Another area for future exploration is refining the lower bound for the low-SNR regime, as Theorem 2 presents loose bounds for this regime.

VI. ACKNOWLEDGMENTS

The authors express gratitude to Prof. Luca Barletta for generously providing the source codes used to compute the information rates of QAM inputs.

APPENDIX A

MATHEMATICAL PRELIMINARIES

Definition 1: A vector random process $\{\underline{\omega}_k\}$ is said to be *circularly symmetric* if

$$\{\underline{\omega}_k\} \sim \{e^{j\Theta_k}\underline{\omega}_k\}, \quad (24)$$

where the process $\{\Theta_k\}$ is $\mathcal{U}[-\pi, \pi)$ and independent of $\{\underline{\omega}_k\}$.

Lemma 1: The input process $\{\underline{\mathbf{x}}_k\}$ that achieves the capacity of the channel (4)–(6) is circularly symmetric.

Proof: The proof follows the same steps as the one in [25, Prop. 7] and relies on the fact that $e^{j\Theta_k}\underline{\mathbf{w}}_k \sim \underline{\mathbf{w}}_k$ for any circularly symmetric random variable $\underline{\mathbf{w}}_k$. \square

Lemma 2 (escape-to-infinity): Fix a real-valued scalar $\xi > 0$. Denote by $C^{(\xi)}(\rho)$ the capacity of the channel (4)–(6) when the input signal is subject to the average-power constraint (8) and to the additional constraint that $|\underline{\mathbf{x}}_k| \geq \xi$ almost surely for all k . Then,

$$C(\rho) = C^{(\xi)}(\rho) + o(1), \quad \rho \rightarrow \infty, \quad (25)$$

with $C(\rho)$ obtained in (7).

Proof: The lemma follows directly from [17, Def. 4.11, Thm. 4.12]. \square

Lemma 3 ([17, Lemma 6.9]): Let \mathbf{v} and τ be two independent real random variables satisfying $\mathbb{E}[|\mathbf{v}|] < \infty$ and $\mathbb{E}[|\tau|] < \infty$. Then,

$$\lim_{\varepsilon \rightarrow 0} h(\mathbf{v} + \varepsilon\tau) = h(\mathbf{v}). \quad (26)$$

Lemma 4 ([17, Lemma 6.15]): For any real random variable $\tau \geq 0$,

$$h(\log \tau) = h(\tau) - \mathbb{E}[\log \tau], \quad (27)$$

and

$$h(\tau^2) = h(\tau) + \mathbb{E}[\log \tau] + \log 2. \quad (28)$$

Lemma 5 ([11, Lemmas 3 and 4]): For any m -dimensional complex random vector $\underline{\omega}$ with $h(\underline{\omega}) > -\infty$, we have

$$h(\underline{\omega}) = h(|\underline{\omega}|^2) + h(\underline{\omega} | |\underline{\omega}|) - m \log 2. \quad (29)$$

In particular, if the elements of $\underline{\omega}$ are circularly symmetric with independent phases, then

$$h(\underline{\omega}) = h(|\underline{\omega}|^2) + m \log \pi. \quad (30)$$

Lemma 6: Let $\omega \sim \mathcal{CN}(0, 1)$ and for a given real β , define $\tau = |\beta + \omega|^2$. Then,

$$h(\tau) = \frac{1}{2} \log \beta^2 + \frac{1}{2} (\log 4\pi e) + o(1), \quad (31)$$

$$\mathbb{E}[\log \tau] = \log \beta^2 + o(1), \quad (32)$$

where the correction term $o(1)$ vanishes when $\beta \rightarrow \infty$.

Proof: Substitute $\nu \rightarrow 2$, $\mathbf{T} \rightarrow 2\tau$, $\mathbf{Z} \rightarrow \sqrt{2}e^{j\Theta}\omega$, $x \rightarrow \sqrt{2}\beta$ in [2, Eqs. (6), (9), and (14)]. Note that in [2], \mathbf{Z} is zero mean with variance 2, therefore we modified the equation to match our assumption that $\omega \sim \mathcal{CN}(0, 1)$. \square

Lemma 7: Let $\omega \sim \mathcal{CN}(0, 1)$ and for any real random variable τ , we can write

$$h(|\tau + \omega|^2 | \tau) \leq \frac{1}{2} \mathbb{E}[\log(2\pi e(1 + 2\tau^2))]. \quad (33)$$

Proof: We can upper-bound $h(|\tau + \omega|^2 | \tau)$ by the entropy of a Gaussian distribution with the same variance. Note that $\text{var}(|\tau + \omega|^2 | \tau) = 1 + 2\tau^2$. The expectation emerges because $h(|\tau + \omega|^2 | \tau) = \mathbb{E}[h(|\tau + \omega|^2 | \tau = \tau)]$ \square

Lemma 8: Let $\Theta \in [-\pi, \pi)$ with $h(\Theta) > -\infty$ and independent of $\omega \sim \mathcal{CN}(0, 1)$; then, for any real random variable τ

$$h(e^{j\Theta}\tau + \omega | \tau) \leq \frac{1}{2} \mathbb{E}[\log(1 + 2\tau^2)] + h(\Theta \mp \underline{\tau + \omega} | \tau) + \frac{1}{2} \log(\pi e) - \frac{1}{2} \log 2. \quad (34)$$

Proof:

$$\begin{aligned} h(e^{j\Theta}\tau + \omega | \tau) &\stackrel{(a)}{=} h(e^{j\Theta}(\tau + \omega) | \tau) \\ &\stackrel{(b)}{=} h(|\tau + \omega|^2 | \tau) + h(\Theta \mp \underline{\tau + \omega} | \tau, |\tau + \omega|) - \log 2 \\ &\stackrel{(c)}{\leq} \frac{1}{2} \mathbb{E}[\log(2\pi e [1 + 2\tau^2])] + h(\Theta \mp \underline{\tau + \omega} | \tau) - \log 2, \end{aligned} \quad (35)$$

where (a) follows because ω is circularly symmetric; (b) is a consequence of Lemma 5; and finally, in (c), we applied Lemma 7 and that conditioning reduces entropy and $h(|\tau + \omega|^2 | \tau)$. Simplifying the RHS of (35) gives (34). \square

Lemma 9: Let $\omega \sim \mathcal{CN}(0, 1)$. For a given real $\beta > 0$ and $\tau > 0$, the conditional distribution of $\underline{\beta + \omega}$ given $|\beta + \omega| = \tau$ is $\mathcal{VM}(0, 2\beta\tau)$.

Proof: Substitute $\epsilon(k) \rightarrow \underline{\beta + \omega}$, $r(k) \rightarrow \tau$, and $\sigma^2/(2A) \rightarrow 1$ in [26, Eq. (12)]. \square

Lemma 10: Let $f_{\theta}^{\text{VM}}(\theta; \mu, 1/\sigma^2)$ and $f_{\theta}^{\text{WN}}(\theta; \mu, \sigma^2)$ denote the pdfs of the von Mises distribution $\mathcal{VM}(\mu, 1/\sigma^2)$ and the wrapped normal distribution $\mathcal{WN}(\mu, \sigma^2)$, respectively. For small σ^2 , the distribution of θ tends to a normal distribution with zero mean $\mu = 0$ and variance of σ^2 such that

$$f_{\theta}^{\text{VM}}(\theta; 0, 1/\sigma^2) - f_{\theta}^{\text{WN}}(\theta; 0, \sigma^2) = O(\sigma), \quad \sigma \rightarrow 0. \quad (36)$$

Proof: See [27] and [28, Eq. 3.5.24]. \square

Lemma 11: For all $0 \leq \alpha \leq 1$ and $0 < x \leq x_0$,

$$(2 + x)^{\alpha} - x^{\alpha} \geq 2\alpha, \quad (37)$$

where $x_0 \approx 0.1770$ is the unique solution $x > 0$ of

$$(2 + x) \log_e(2 + x) - x \log_e x - 2 = 0. \quad (38)$$

Proof: We define for any fixed $0 < x \leq x_0$

$$\zeta(\alpha) = (2 + x)^{\alpha} - x^{\alpha} - 2\alpha \quad (39)$$

and calculate its derivatives

$$\zeta'(\alpha) = (2 + x)^{\alpha} \log_e(2 + x) - x^{\alpha} \log_e x - 2, \quad (40)$$

$$\zeta''(\alpha) = (2 + x)^{\alpha} (\log_e(2 + x))^2 - x^{\alpha} (\log_e x)^2, \quad (41)$$

which are continuous and differentiable for $x > 0$. The equation $\zeta''(\alpha) = 0$ has a unique solution

$$\alpha = \bar{\alpha} = 2 \frac{\log_e \left(\frac{-\log_e x}{\log_e(2+x)} \right)}{\log_e \left(\frac{2+x}{x} \right)} < 1, \quad (42)$$

where the inequality follows because $\zeta''(\alpha)$ is increasing and $\zeta''(1) > 0$. Hence, $\zeta''(\alpha) \leq 0$ for $0 \leq \alpha \leq \bar{\alpha}$ and $\zeta''(\alpha) \geq 0$ for $\bar{\alpha} \leq \alpha \leq 1$. These properties will now be used to prove that $\zeta(\alpha) \geq 0$ in both intervals.

We first consider $\alpha = 1$. Here, $\zeta(1) = 0$ and

$$\zeta'(1) = (2 + x) \log_e(2 + x) - x \log_e x - 2. \quad (43)$$

This function increases monotonically for all $x > 0$ and equals zero for $x = x_0$ by (38). Hence, $\zeta'(1) \leq 0$ for $0 < x \leq x_0$.

We next consider $\bar{\alpha} \leq \alpha \leq 1$. Since $\zeta(\alpha)$ is convex in this interval, it is not less than its tangent at $\alpha = 1$, i.e.,

$$\zeta(\alpha) \geq \zeta(1) + \zeta'(1)(\alpha - 1) \quad (44)$$

$$\geq 0. \quad (45)$$

In $0 \leq \alpha \leq \bar{\alpha}$, finally, $\zeta(\alpha)$ is concave and by Jensen's equality not less than its secant, i.e.,

$$\zeta(\alpha) \geq \frac{\bar{\alpha} - \alpha}{\bar{\alpha}} \zeta(0) + \frac{\alpha}{\bar{\alpha}} \zeta(\bar{\alpha}) \quad (46)$$

$$\geq 0, \quad (47)$$

because $\zeta(0) = 0$ and $\zeta(\bar{\alpha}) \geq 0$ by (45).

Together, (45) and (47) prove (37) for all $0 \leq \alpha \leq 1$. \square

Lemma 12: For all $0 < \alpha \leq 1$ and $0 < x \leq x_0$,

$$\Gamma(\alpha, x) \geq \Gamma(1, x), \quad (48)$$

where $x_0 \approx 0.1770$ was defined in Lemma 11.

Proof: For all $0 < \alpha \leq 1$ and $0 < x \leq x_0$, from [29, Ch. 8, Eq. (8.10.10)] and that $\Gamma(1, x) = e^{-x}$ we have

$$x^{1-\alpha} e^x \Gamma(\alpha, x) \geq \frac{x}{2\alpha} \left(\left(1 + \frac{2}{x}\right)^\alpha - 1 \right). \quad (49)$$

With some basic mathematical operations, we can rewrite (49) as

$$\begin{aligned} \Gamma(\alpha, x) &\geq e^{-x} \frac{(x+2)^\alpha - x^\alpha}{2\alpha} \\ &\stackrel{(a)}{\geq} e^{-x} \\ &= \Gamma(1, x), \end{aligned} \quad (50)$$

where in (a) we utilized Lemma 11. \square

Lemma 13: Let the random scalar $\mathbf{r} \sim \mathcal{G}_{\text{tr}}(\mu, \alpha, \gamma)$ where $\mu > 0$, $\alpha > 0$, and $\gamma > 0$. Also, define

$$J(\alpha, \gamma) = \alpha + \frac{e^{-\gamma} \gamma^\alpha}{\Gamma(\alpha, \gamma)}. \quad (51)$$

Then,

$$\begin{aligned} \mathbb{E}[\mathbf{r}] &= \mu \frac{\Gamma(\alpha + 1, \gamma)}{\Gamma(\alpha, \gamma)} \\ &= \mu J(\alpha, \gamma). \end{aligned} \quad (52)$$

Proof: Using (1) and setting $M = 1$ to get the pdf for a scalar random variable, we can write

$$\begin{aligned}
\mathbb{E}[\mathbf{r}] &= \frac{1}{\Gamma(\alpha, \gamma)} \int_{\mu\gamma}^{\infty} e^{-\frac{r}{\mu}} \mu^{-\alpha} r^{\alpha} dr \\
&\stackrel{(a)}{=} \frac{\mu}{\Gamma(\alpha, \gamma)} \int_{\gamma}^{\infty} e^{-u} u^{\alpha} du, \\
&\stackrel{(b)}{=} \mu \frac{\Gamma(\alpha + 1, \gamma)}{\Gamma(\alpha, \gamma)} \\
&\stackrel{(c)}{=} \mu \left(\alpha + \frac{e^{-\gamma} \gamma^{\alpha}}{\Gamma(\alpha, \gamma)} \right) \\
&= \mu J(\alpha, \gamma), \tag{53}
\end{aligned}$$

where in (a) we employed the change of variable technique by defining $u = r/\mu$, in (b) we used that $\Gamma(\alpha + 1, \gamma) = \int_{\gamma}^{\infty} e^{-u} u^{\alpha} du$, and in (c) we used that $\Gamma(\alpha + 1, \gamma) = \alpha\Gamma(\alpha, \gamma) + e^{-\gamma} \gamma^{\alpha}$. \square

Lemma 14: For any $m \in \{0, \dots, M - 1\}$ and any $0 \leq x \leq x_{\max}$, let

$$c_m(x) = \frac{W_L(x^{\alpha_m^*} \log_e x)}{\log_e x} = \frac{x^{\alpha_m^*}}{e^{W_L(x^{\alpha_m^*} \log_e x)}}, \tag{54}$$

where α_m^* defined in (18). Moreover, $W_L(x)$ is the principal branch of the Lambert W function, which is defined for any $x \geq -e^{-1}$ by $e^{W_L(x)} W_L(x) = x$ and $W_L(x) \geq -1$ [30], and $x_{\max} \approx 0.00471$ is the smallest $x > 0$ for which

$$x^{\alpha_m^*} \log_e x \geq -\frac{1}{e}. \tag{55}$$

Then, we have

$$x^{c_m(x)} = \frac{x^{\alpha_m^*}}{c_m(x)}. \tag{56}$$

Proof:

$$\begin{aligned}
x^{c_m(x)} &= e^{\log_e(x) c_m(x)} \\
&= e^{W_L(x^{\alpha_m^*} \log_e(x))} \\
&\stackrel{(a)}{=} \frac{x^{\alpha_m^*} \log_e(x)}{W_L(x^{\alpha_m^*} \log_e(x))} \\
&= \frac{x^{\alpha_m^*}}{c_m(x)}, \tag{57}
\end{aligned}$$

where (a) follows from the definition of the Lambert W function. \square

Lemma 15: Let $\theta \in [-\pi, \pi)$ be a random variable with pdf

$$g_{\theta}(\theta) = f_{\theta}^{\text{WN}}(\theta; 0, \sigma^2) + O(\sigma), \quad \sigma \rightarrow 0, \tag{58}$$

where $f_{\theta}^{\text{WN}}(\theta; 0, \sigma^2)$ denotes the zero-mean wrapped normal distribution with variance σ^2 . Then,

$$h(\theta) = \frac{1}{2} \log(2\pi e \sigma^2) + O(\sigma), \quad \sigma \rightarrow 0. \tag{59}$$

Proof: The pdf of a zero-mean wrapped normal distribution with variance σ^2 is defined as

$$f_{\boldsymbol{\theta}}^{\text{WN}}(\theta; 0, \sigma^2) = \frac{1}{\sqrt{2\pi\sigma^2}} \sum_{l=-\infty}^{\infty} \exp\left(-\frac{(\theta - 2\pi l)^2}{2\sigma^2}\right), \quad (60)$$

where $\theta \in [-\pi, \pi)$. Now let

$$f_{\text{G}}(\theta) = \frac{1}{\sqrt{2\pi\sigma^2}} \exp\left(-\frac{\theta^2}{2\sigma^2}\right), \quad -\infty \leq \theta \leq \infty. \quad (61)$$

For any $\theta \in [-\pi, \pi)$,

$$\begin{aligned} f_{\boldsymbol{\theta}}^{\text{WN}}(\theta; 0, \sigma^2) - f_{\text{G}}(\theta) &= \frac{1}{\sqrt{2\pi\sigma^2}} \sum_{\substack{l=-\infty \\ l \neq 0}}^{\infty} \exp\left(-\frac{(\theta - 2\pi l)^2}{2\sigma^2}\right) \\ &\stackrel{(a)}{\leq} \frac{2}{\sqrt{2\pi\sigma^2}} \sum_{l=1}^{\infty} \exp\left(-\frac{\pi^2 l^2}{2\sigma^2}\right) \\ &= O\left(\frac{1}{\sigma} \exp\left(-\frac{\pi^2}{2\sigma^2}\right)\right), \end{aligned} \quad (62)$$

where (a) follows since $(\theta - 2\pi l)^2 \geq \pi^2 l^2 \geq \pi^2 l$ for $|\theta| \leq \pi$ and $l \geq 1$. Now for $\theta \in [-\pi, \pi)$, we can write

$$\begin{aligned} g_{\boldsymbol{\theta}}(\theta) &= f_{\text{G}}(\theta) + O\left(\frac{1}{\sigma} \exp\left(-\frac{\pi^2}{2\sigma^2}\right)\right) + O(\sigma) \\ &= f_{\text{G}}(\theta) + O(\sigma), \end{aligned} \quad (63)$$

where the last equality holds since $\exp(-\pi^2/(2\sigma^2))/\sigma$ has faster decay than σ as $\sigma \rightarrow 0$.

Defining the entropy of $\boldsymbol{\theta}$ as

$$h(\boldsymbol{\theta}) = - \int_{-\pi}^{\pi} g_{\boldsymbol{\theta}}(\theta) \log g_{\boldsymbol{\theta}}(\theta) d\theta, \quad (64)$$

we can write

$$\begin{aligned} h(\boldsymbol{\theta}) &= - \int_{-\pi}^{\pi} (f_{\text{G}}(\theta) + O(\sigma)) \log g_{\boldsymbol{\theta}}(\theta) d\theta \\ &\stackrel{(a)}{=} - \int_{-\pi}^{\pi} f_{\text{G}}(\theta) \log g_{\boldsymbol{\theta}}(\theta) d\theta + O(\sigma) \\ &= - \int_{-\pi}^{\pi} f_{\text{G}}(\theta) \left(\log f_{\text{G}}(\theta) + \log \frac{g_{\boldsymbol{\theta}}(\theta)}{f_{\text{G}}(\theta)} \right) d\theta + O(\sigma) \\ &= - \int_{-\pi}^{\pi} f_{\text{G}}(\theta) \log f_{\text{G}}(\theta) d\theta \\ &\quad - \int_{-\pi}^{\pi} f_{\text{G}}(\theta) \log \frac{g_{\boldsymbol{\theta}}(\theta)}{f_{\text{G}}(\theta)} d\theta + O(\sigma), \end{aligned} \quad (65)$$

where in (a) we used the fact that $f_{\text{G}}(\theta) > 0$ for all $\theta \in [-\pi, \pi)$ and $\sigma \geq 0$.

The first term on the RHS of (65) can be evaluated as

$$\begin{aligned} - \int_{-\pi}^{\pi} f_G(\theta) \log f_G(\theta) d\theta &= \left(1 - \operatorname{erfc}\left(\frac{\pi}{\sqrt{2\sigma^2}}\right)\right) \frac{\log(2\pi e\sigma^2)}{2} - \sqrt{\frac{\pi}{2\sigma^2}} \exp\left(-\frac{\pi^2}{2\sigma^2}\right) \\ &= \frac{1}{2} \log(2\pi e\sigma^2) + O\left(\frac{1}{\sigma} \exp\left(-\frac{\pi^2}{2\sigma^2}\right)\right). \end{aligned} \quad (66)$$

The second term on the RHS of (65) can be written as

$$\begin{aligned} - \int_{-\pi}^{\pi} f_G(\theta) \log\left(\frac{g_{\theta}(\theta)}{f_G(\theta)}\right) d\theta &\stackrel{(a)}{\leq} \int_{-\pi}^{\pi} f_G(\theta) \left(1 - \frac{g_{\theta}(\theta)}{f_G(\theta)}\right) d\theta \\ &= \int_{-\pi}^{\pi} (f_G(\theta) - g_{\theta}(\theta)) d\theta \\ &\stackrel{(b)}{=} \int_{-\pi}^{\pi} O(\sigma) d\theta \\ &= O(\sigma), \end{aligned} \quad (67)$$

where in (a) we utilize that $-\log(x) \leq 1 - x$ for $x > 0$. We can do this because both $g_{\theta}(\theta) > 0$ and $f_G(\theta) > 0$; (b) directly follows from (63).

Combining (67) and (66) into (65) we get

$$h(\theta) = \frac{1}{2} \log(2\pi e\sigma^2) + O(\sigma), \quad (68)$$

and the proof is complete. \square

APPENDIX B

PROOF OF CAPACITY UPPER AND LOWER BOUNDS

This section is dedicated to proving capacity upper and lower bounds in Theorems 1 and 2.

To establish the upper bound in Theorem 1, we adopt the duality approach, leveraging that any output distribution provides an upper bound on the capacity. Specifically, we focus on a family of circularly symmetric distributions where the squared magnitude of the outputs follows the gamma distribution $\mathcal{G}_{\text{tr}}(\mu > 0, \underline{\alpha} > 0, 0)$.

On the other hand, for the lower bound in Theorem 2, we rely on the insight that any input distribution provides a lower bound on the capacity. Consequently, we introduce a circularly symmetric input distribution with the squared magnitude of the inputs following a truncated gamma distribution $\mathcal{G}_{\text{tr}}(\mu > 0, \underline{\alpha} > 0, \gamma > 0)$.

Both theorems are proven under the assumption of circularly symmetric input distributions, as Lemma 1 establishes that the capacity-achieving distribution for MIMO phase-noise channels (4)–(6) is indeed circularly symmetric.

B.1 Proof of 1 (Upper Bound)

The following lemma characterizes an upper bound on the capacity of the channel (4)–(6) and serves as starting points for formulating an upper bound on the capacity of a MIMO phase-noise channel, whether the phase noises are independent or correlated.

Lemma 16: The capacity of the channel (4)–(6) under the power constraint (8) can be upper-bounded as

$$C(\rho) \leq \sup_{\mathcal{Q}_{\underline{\mathbf{x}}_1}} \left\{ I(\underline{\mathbf{x}}_1; \underline{\mathbf{y}}_1) + I(\underline{\mathbf{y}}_1; \underline{\boldsymbol{\theta}}_0 | \underline{\mathbf{x}}_1) \right\}, \quad (69)$$

where the supremum is over all probability distributions $\mathcal{Q}_{\underline{\mathbf{x}}_1}$ on $\underline{\mathbf{x}}_1$ that satisfy the power constraint $\mathbb{E}[\|\underline{\mathbf{x}}_1\|^2] \leq \rho$.

Proof: See Appendix D.1. □

We start by upper-bounding each term on the RHS of (69). Thanks to Lemma 1, our focus can be narrowed down to input processes with circular symmetry. Specifically, we will examine $\underline{\mathbf{x}}_k$ whose amplitude $|\underline{\mathbf{x}}_k|$ and phase $\angle \underline{\mathbf{x}}_k$ are independent of each other.

In the next lemma, we utilize the duality approach [17, Theorem. 5.1] to upper-bound $I(\underline{\mathbf{x}}_1; \underline{\mathbf{y}}_1)$.

Lemma 17: For channel (4)–(6) and for any circularly symmetric distribution $\mathcal{Q}_{\underline{\mathbf{x}}_1}$ on $\underline{\mathbf{x}}_1$ that satisfies $\mathbb{E}[\|\underline{\mathbf{x}}_1\|] \leq \rho$, $\underline{\alpha} = (\alpha_0, \dots, \alpha_{M-1}) > 0$, and $\lambda \geq 0$, we have

$$I(\underline{\mathbf{x}}_1; \underline{\mathbf{y}}_1) \leq \alpha_\Sigma \log \left(\frac{\rho + M}{\alpha_\Sigma} \right) + d_{\lambda, \underline{\alpha}} + \mathbb{E} [R_{\lambda, \underline{\alpha}}(\rho, |\underline{\mathbf{x}}_1|)], \quad (70)$$

where

$$d_{\lambda, \underline{\alpha}} = \lambda - (M - 2) \log e + \sum_{m=0}^{M-1} \log \Gamma(\alpha_m), \quad (71)$$

and α_Σ and $R_{\lambda, \underline{\alpha}}(\cdot)$ are defined in (10) and (11), respectively.

Proof: See Appendix D.2. □

It is rather challenging to characterize $I(\underline{\mathbf{y}}_1; \underline{\boldsymbol{\theta}} | \underline{\mathbf{x}}_1)$ for $M > 2$. In the following lemma, we present a precise characterization of this term specifically for the case of $M = 2$ and provide a looser upper bound when $M > 2$.

Lemma 18: For channel (4)–(6) and for any circularly symmetric $\mathcal{Q}_{\underline{\mathbf{x}}_1}$ on $\underline{\mathbf{x}}_1$ that satisfies $\mathbb{E}[\|\underline{\mathbf{x}}_1\|] \leq \rho$, the second term on the RHS of (69) is

$$I(\underline{\mathbf{y}}_1; \underline{\boldsymbol{\theta}}_0 | \underline{\mathbf{x}}_1) \leq 2 \log(2\pi) + F(M, |\underline{\mathbf{x}}_1|, \underline{\boldsymbol{\Delta}}_1^c, \underline{\boldsymbol{\Delta}}_1^r), \quad (72)$$

where $F(\cdot)$ is defined in (12). Here, $\underline{\boldsymbol{\Delta}}_1^c \sim \mathcal{WN}(0, \sigma_c^2)$ and $\underline{\boldsymbol{\Delta}}_1^r \sim \mathcal{WN}(0, \sigma_r^2)$ are independent.

Proof: See Appendix D.3. □

Substituting (72) and (70) into (69), we obtain

$$C(\rho) \leq \alpha_\Sigma \log \left(\frac{\rho + M}{\alpha_\Sigma} \right) + 2 \log(2\pi) + d_{\lambda, \alpha} + \sup_{\mathcal{Q}_{|\mathbf{x}_1|}} \{ \mathbb{E} [R_{\lambda, \alpha}(\rho, |\mathbf{x}_1|)] + F(M, |\mathbf{x}_1|, \mathbf{\Delta}_1^c, \mathbf{\Delta}_1^r) \}, \quad (73)$$

where the supremum over $\mathcal{Q}_{\mathbf{x}_1}$ is replaced with supremum over $\mathcal{Q}_{|\mathbf{x}_1|}$ that satisfies the power constraint $\mathbb{E}[\|\mathbf{x}_1\|^2] \leq \rho$.

Defining a real deterministic vector $\underline{s} \geq 0$, we can write

$$C(\rho) \leq \alpha_\Sigma \log \left(\frac{\rho + M}{\alpha_\Sigma} \right) + 2 \log(2\pi) + d_{\lambda, \alpha} + \max_{\underline{s} \geq 0} \{ R_{\lambda, \alpha}(\rho, \underline{s}) + F(M, \underline{s}, \mathbf{\Delta}^c, \mathbf{\Delta}^r) \}, \quad (74)$$

which follows as the supremum over all $\mathcal{Q}_{|\mathbf{x}_1|}$ is upper-bounded by removing the power constraint and maximizing over all deterministic $\underline{s} \geq 0$. For convenience, the time index is dropped and all the random quantities are replaced by timeless random variables with the same distributions, i.e., $\mathbf{v}_1 \rightarrow \mathbf{v}$, $\mathbf{\Delta}_1^c \rightarrow \mathbf{\Delta}^c$, $\mathbf{\Delta}_1^r \rightarrow \mathbf{\Delta}^r$ and $\mathbf{z}_{1,m} \rightarrow \mathbf{z}_m$ for all m . Replacing (71) into (74) concludes the proof of Theorem 1.

B.2 Proof of 2 (Lower Bound)

The following lemma characterizes a lower bound on the capacity of the channel (4)–(6) and it holds whether the phase noises are independent or correlated.

Lemma 19: The capacity of the channel (4)–(6) under the power constraint (8) can be lower-bounded as

$$C(\rho) \geq I(\mathbf{x}_2; \mathbf{y}_2 | \boldsymbol{\theta}_1) - I(\mathbf{x}_2; \boldsymbol{\theta}_1 | \mathbf{x}_1, \mathbf{y}_1, \mathbf{y}_2), \quad (75)$$

for any distribution on \mathbf{x}_1 and \mathbf{x}_2 that fulfill $\mathbb{E}[\|\mathbf{x}_1\|^2] \leq \rho$ and $\mathbb{E}[\|\mathbf{x}_2\|^2] \leq \rho$.

Proof: See Appendix D.4. □

To derive the lower bound, we use Lemma 19 and start by examining the two terms on the RHS of (75) separately. We can rewrite the first term as

$$I(\mathbf{x}_2; \mathbf{y}_2 | \boldsymbol{\theta}_1) = h(\mathbf{y}_2 | \boldsymbol{\theta}_1) - h(\mathbf{y}_2 | \mathbf{x}_2, \boldsymbol{\theta}_1). \quad (76)$$

Lemma 1 allows us to narrow our attention to input processes exhibiting circular symmetry. Here, we consider a circularly symmetric input vector with independent elements. Thus, the first term on the RHS

of (76) can be bounded as

$$\begin{aligned}
h(\underline{\mathbf{y}}_2 | \underline{\boldsymbol{\theta}}_1) &\geq h(\underline{\mathbf{y}}_2 | \underline{\mathbf{w}}_2, \underline{\boldsymbol{\theta}}_1) \\
&= h(e^{j\boldsymbol{\theta}_2} \circ \underline{\mathbf{x}}_2 | \underline{\boldsymbol{\theta}}_1) \\
&\stackrel{(a)}{=} h(\underline{\mathbf{x}}_2) \\
&\stackrel{(b)}{=} \sum_{m=0}^{M-1} \left(h(|\mathbf{x}_{2,m}|^2) + h(\angle \underline{\mathbf{x}}_{2,m} | |\mathbf{x}_{2,m}|) - \log 2 \right) \\
&\stackrel{(c)}{=} M \log \pi + \sum_{m=0}^{M-1} h(|\mathbf{x}_{2,m}|^2) \tag{77}
\end{aligned}$$

$$= M \log \pi + h(|\underline{\mathbf{x}}_2|^2), \tag{78}$$

where (a) holds since $\underline{\mathbf{x}}_2$ is circularly symmetric and rotation does not change its distribution, i.e., $e^{j\boldsymbol{\theta}_2} \circ \underline{\mathbf{x}}_2 \sim \underline{\mathbf{x}}_2$; in (b) we applied Lemma 5 and that the squared amplitudes $|\mathbf{x}_{2,m}|^2$ are i.i.d. for any m ; in (c) we used that the phases $\angle \underline{\mathbf{x}}_{2,m} \sim \mathcal{U}[-\pi, \pi)$ independently of the amplitudes $|\mathbf{x}_{2,m}|$.

Continuing with the chain rule, we can express the second term on the RHS of (76) as

$$h(\underline{\mathbf{y}}_2 | \underline{\mathbf{x}}_2, \underline{\boldsymbol{\theta}}_1) \leq h(\{\mathbf{y}_{2,m}\}_0^1 | \underline{\mathbf{x}}_2, \underline{\boldsymbol{\theta}}_1) + h(\{\mathbf{y}_{2,m}\}_2^{M-1} | \underline{\mathbf{x}}_2, \{\mathbf{y}_{2,m}\}_0^1), \tag{79}$$

where the inequality follows as conditioning reduces entropy. The following lemmas upper-bound both terms on the RHS of (79).

Lemma 20: The first term on the RHS of (79) can be upper-bounded as

$$\begin{aligned}
h(\{\mathbf{y}_{2,m}\}_0^1 | \underline{\mathbf{x}}_2, \underline{\boldsymbol{\theta}}_1) &\leq \log(\pi e) - \log 2 + \frac{1}{2} \mathbb{E} \left[\log \left(1 + 2 |\mathbf{x}_{2,0}|^2 \right) \right] + \frac{1}{2} \mathbb{E} \left[\log \left(1 + 2 |\mathbf{x}_{2,1}|^2 \right) \right] \\
&\quad + h(\{\Delta_2^c \mp m \Delta_2^r \mp \angle |\mathbf{x}_{2,m}| + \mathbf{z}_{2,m}\}_0^1 | |\underline{\mathbf{x}}_2|, \{\mathbf{y}_{2,m}\}_0^1), \tag{80}
\end{aligned}$$

where $|\mathbf{y}_{2,m}| = ||\mathbf{x}_{2,m}| + \mathbf{z}_{2,m}|$ and $\mathbf{z}_{2,m} \sim \mathcal{CN}(0, 1)$.

Proof: See Appendix D.5. □

Lemma 21: The second term on the RHS of (79) can be bounded as

$$h(\{\mathbf{y}_{2,m}\}_2^{M-1} | \underline{\mathbf{x}}_2, \{\mathbf{y}_{2,m}\}_0^1) \leq (M-2) \log(\pi e) + \sum_{m=2}^{M-1} \mathbb{E}[g(m, |\underline{\mathbf{x}}_2|)], \tag{81}$$

where $g(\cdot)$ is defined in (14).

Proof: See Appendix D.6. □

Substituting (81) and (80) into (79) gives

$$\begin{aligned}
h(\underline{\mathbf{y}}_2 | \underline{\mathbf{x}}_2, \underline{\boldsymbol{\theta}}_1) &\leq (M-1) \log(\pi e) - \log 2 + \frac{1}{2} \mathbb{E} \left[\log \left(1 + 2 |\mathbf{x}_{2,0}|^2 \right) \right] + \frac{1}{2} \mathbb{E} \left[\log \left(1 + 2 |\mathbf{x}_{2,1}|^2 \right) \right] \\
&\quad + h(\{\Delta_2^c \mp m \Delta_2^r \mp \angle |\mathbf{x}_{2,m}| + \mathbf{z}_{2,m}\}_0^1 | |\underline{\mathbf{x}}_2|, \{\mathbf{y}_{2,m}\}_0^1) + \sum_{m=2}^{M-1} \mathbb{E}[g(m, |\underline{\mathbf{x}}_2|)]. \tag{82}
\end{aligned}$$

Substituting (82) and (78) in (76) gives

$$\begin{aligned}
I(\underline{\mathbf{x}}_2; \underline{\mathbf{y}}_2 | \underline{\boldsymbol{\theta}}_1) &\geq \log(2\pi) - (M-1) \log e + h(|\underline{\mathbf{x}}_2|^2) \\
&\quad - \frac{1}{2} \mathbb{E} \left[\log \left(1 + 2 |\mathbf{x}_{2,0}|^2 \right) \right] - \frac{1}{2} \mathbb{E} \left[\log \left(1 + 2 |\mathbf{x}_{2,1}|^2 \right) \right] \\
&\quad - h \left(\left\{ \Delta_2^c \mp m \Delta_2^r \mp \sqrt{|\mathbf{x}_{2,m}| + \mathbf{z}_{2,m}} \right\}_0^1 | |\underline{\mathbf{x}}_2|, \{|\mathbf{y}_{2,m}|\}_0^1 \right) - \sum_{m=2}^{M-1} \mathbb{E}[g(m, |\underline{\mathbf{x}}_2|)]. \quad (83)
\end{aligned}$$

To this point, (83) provides a lower bound for the first term on the RHS of (75). To finalize the derivation of the lower bound, the following lemma provides an upper bound on the second term on the RHS of (75).

Lemma 22: The second term on the RHS of (75) can be upper-bounded as

$$I(\underline{\mathbf{x}}_2; \underline{\boldsymbol{\theta}}_1 | \underline{\mathbf{x}}_1, \underline{\mathbf{y}}_1, \underline{\mathbf{y}}_2) \leq h \left(\left\{ \Delta_2^c \mp m \Delta_2^r \mp \sqrt{|\mathbf{x}_{2,m}| + \mathbf{z}_{2,m}} \right\}_0^1 | |\underline{\mathbf{x}}_2|, \{|\mathbf{y}_{2,m}|\}_0^1 \right) - h(\Delta_2^c, \Delta_2^r), \quad (84)$$

where $|\mathbf{y}_{2,m}| = \sqrt{|\mathbf{x}_{2,m}| + \mathbf{z}_{2,m}}$ and $\mathbf{z}_{2,m} \sim \mathcal{CN}(0, 1)$. Moreover, $\Delta_2^c \sim \mathcal{WN}(0, \sigma_c^2)$ and $\Delta_2^r \sim \mathcal{WN}(0, \sigma_r^2)$ are independent of all the other random variables.

Proof: See Appendix D.7. □

For sufficiently large $|\underline{\mathbf{x}}_2|$, (84) can be made arbitrarily close to zero. This property will be used in Section C.1 to obtain a high-SNR lower bound on the capacity.

Finally, substituting (84) and (83) into (75) results in the desired lower bound (13) on the capacity. Note that we defined $\underline{\mathbf{s}} = |\underline{\mathbf{x}}_2|$ and replaced all the random quantities with timeless random variables with the same distributions (i.e., $\Delta_2^c \rightarrow \Delta^c$, $\Delta_2^r \rightarrow \Delta^r$, $\mathbf{z}_2 \rightarrow \mathbf{z}$, $|\underline{\mathbf{x}}_2| \rightarrow \underline{\mathbf{s}}$).

APPENDIX C

HIGH-SNR CAPACITY BOUNDS

This section is dedicated to the proof of the high-SNR bounds in Section III-B. For the upper bound, we exploit the insight in Lemma 2 that at high SNRs, the capacity can be achieved using an input distribution that escapes to infinity. To establish the lower bound, we choose a particular input distribution that escapes to infinity as the SNR approaches infinity.

C.1 Proof of 3 (High-SNR Upper Bound)

Based on Lemma 2, the high-SNR behavior of $C(\rho)$ does not change under the additional constraint that the support of the amplitude of each element of the input vector lies outside an arbitrary radius. Hence, we present the high-SNR behavior of a modified version of the upper bound presented in Theorem 1 under the additional constraint that $|\underline{\mathbf{x}}_k| \geq \xi$ for all k and any $0 < \xi < \sqrt{\rho/M}$.

Set $\lambda = \lambda^* = (M - 1) \log e$ and $\underline{\alpha} = \underline{\alpha}^*$ defined in (18), which results in $\alpha_\Sigma = M - 1$ and $d_{\lambda^*, \underline{\alpha}^*} = \log(\pi e)$. We define $C^{(\xi)}(\rho)$ similar to (7)–(8) with the additional constraint that $|\underline{\mathbf{x}}_k| \geq \xi$ for all k . Then, a similar relation to (69) can be obtained where the supremum is over all distributions $\mathcal{Q}_{\underline{\mathbf{x}}}$ such that $\mathbb{E}[\|\underline{\mathbf{x}}_1\|] \leq \rho$ and $|\underline{\mathbf{x}}_1| \geq \xi$, and from there by applying Lemma 17 and Lemma 18, we obtain $C^{(\xi)}(\rho) \leq U^{(\xi)}(\rho)$, where

$$U^{(\xi)}(\rho) = (M - 1) \log \left(\frac{\rho + M}{M - 1} \right) + \log(\pi e) + 2 \log(2\pi) + \max_{\underline{s} \geq \xi} \{ R_{\lambda^*, \underline{\alpha}^*}(\rho, \underline{s}) + F(M, \underline{s}, \mathbf{\Delta}^c, \mathbf{\Delta}^r) \}. \quad (85)$$

Here, the supremum over all $\mathcal{Q}_{\underline{\mathbf{x}}_1}$ satisfying $|\underline{\mathbf{x}}_1| \geq \xi$ is upper-bounded by removing the power constraint and maximizing over all deterministic $\underline{s} \geq \xi$.

The following lemma helps to characterize the high-SNR behavior of (85).

Lemma 23: For any finite ρ

$$\lim_{\underline{s} \rightarrow \infty} R_{\lambda^*, \underline{\alpha}^*}(\rho, \underline{s}) = -\log(4\pi e), \quad (86)$$

and

$$\lim_{\underline{s} \rightarrow \infty} F(M, \underline{s}, \mathbf{\Delta}^c, \mathbf{\Delta}^r) = -h(\mathbf{\Delta}^c, \mathbf{\Delta}^r), \quad (87)$$

where $\underline{s} \rightarrow \infty$ stands for $s_m \rightarrow \infty$ for all $m \in \{0, \dots, M - 1\}$.

Proof: See Appendix D.8. □

Choosing⁵ $\xi < \sqrt{\rho/M}$ as a function of ρ such that $\xi \rightarrow \infty$ as $\rho \rightarrow \infty$, we obtain from (85) and Lemma 23

$$U^{(\xi)}(\rho) = U_{\text{hsnr}}(\rho), \quad (88)$$

where $U_{\text{hsnr}}(\rho)$ is defined in Theorem 3. Finally, using (88) and recalling from Lemma 2 that $C^{(\xi)}(\rho) = C(\rho) + o(1)$, we can write

$$C(\rho) \leq U_{\text{hsnr}}(\rho), \quad (89)$$

which completes the proof of Theorem 3.

C.2 Proof of 4 (High-SNR Lower Bound)

Here, we characterize the high-SNR characteristics of the lower bound by selecting a particular distribution for \underline{s} in Theorem 2. We opt for the truncated gamma distribution for \underline{s} based on the rationale that in the high-SNR regime, the output can be considered as a rotated version of the input. Given that

⁵For instance, setting $\xi = \sqrt{\rho}/M$ satisfies the required conditions. Note that certain other functions will give the same result.

we employed the truncated gamma distribution for the squared amplitude of the output to derive the high-SNR upper bound, it is reasonable to employ the same distribution for the squared amplitude of the input. Furthermore, the truncated gamma distribution serves as a versatile representation encompassing various well-known distributions.

Let $\mu = \rho/(M - 1)$, $\gamma > 0$, and $\underline{\alpha}'(\gamma) \geq 0$ and take $\underline{\mathbf{s}} \sim \mathcal{SG}_{\text{tr}}(\mu, \underline{\alpha}'(\gamma), \gamma)$. Using Lemma 13 we can write

$$\begin{aligned} \mathbb{E}[\|\underline{\mathbf{s}}\|^2] &= \sum_{m=0}^{M-1} \mathbb{E}[|\mathbf{s}_m|^2] \\ &= \mu \sum_{m=0}^{M-1} J(\alpha'_m(\gamma), \gamma), \end{aligned} \quad (90)$$

where $J(\cdot)$ is defined in (51). The distribution parameters γ and $\underline{\alpha}'(\gamma)$ must be selected such that the power constraint $\mathbb{E}[\|\underline{\mathbf{s}}\|^2] \leq \rho$ is satisfied.

The proof hinges on the choice of $\underline{\alpha}'(\gamma)$ and γ as a function of ρ such that (90) is satisfied, and as $\rho \rightarrow \infty$, we have $\rho\gamma \rightarrow \infty$, $\gamma \rightarrow 0$, and $\underline{\alpha}'(\gamma) \rightarrow \underline{\alpha}^*$ where $\underline{\alpha}^*$ is defined in (18). Here, we select⁶

$$\alpha'_m(\gamma) = \alpha_m^* - c_m(\gamma), \quad (91)$$

where α_m^* and $c_m(\gamma)$ are defined in (18) and (54), respectively. We also choose⁷

$$\gamma = x_{\max} \cdot \begin{cases} 1/\sqrt{\rho}, & \rho \geq 1, \\ \rho, & 0 < \rho < 1, \end{cases} \quad (92)$$

which results in having $0 < \gamma \leq x_{\max}$ and as $\rho \rightarrow \infty$ we have $\rho\gamma \rightarrow \infty$ and $\gamma \rightarrow 0$.

Lemma 24: For $\underline{\alpha}'(\gamma)$ defined in (91) and for any $0 \leq \gamma \leq x_{\max}$ where $x_{\max} \approx 0.00471$ is defined in Lemma 14, we have

$$J(\alpha'_m(\gamma), \gamma) \leq \alpha_m^*, \quad (93)$$

and

$$\lim_{\gamma \rightarrow 0^+} \alpha'_m(\gamma) = \alpha_m^*. \quad (94)$$

Proof: See Appendix D.9. □

Substituting (93) into (90) leads to $\mathbb{E}[\|\underline{\mathbf{s}}\|^2] \leq \rho$. Moreover, (94) shows that $\underline{\alpha}'(\gamma)$ converges to $\underline{\alpha}^*$ element-wise as $\gamma \rightarrow 0$.

⁶Any other $\underline{\alpha}'(\gamma)$ that lead to $\mathbb{E}[\|\underline{\mathbf{s}}\|^2] \leq \rho$ and $\lim_{\gamma \rightarrow 0^+} \underline{\alpha}'(\gamma) = \underline{\alpha}^*$ will give the same result.

⁷Many other functions will give the same result.

Note that with the chosen truncated distribution we have

$$|\underline{\mathbf{s}}| > \sqrt{\mu\gamma} = \sqrt{\rho\gamma/(M-1)} \quad (95)$$

from (1); thus, $\Pr\{\underline{\mathbf{s}} \geq \sqrt{\mu\gamma}\} = 1$.

Using Lemma 3 and that the phases $\underline{\mathbf{s}}_0 + \mathbf{z}_0 \rightarrow 0$ and $\underline{\mathbf{s}}_1 + \mathbf{z}_1 \rightarrow 0$, with probability 1 as $\rho \rightarrow \infty$, we can write

$$h(\{\Delta^c \mp m\Delta^r \mp \underline{\mathbf{s}}_m + \mathbf{z}_m\}_0^1 | \underline{\mathbf{s}}, \{\|\mathbf{s}_m + \mathbf{z}_m\|_0^1\}) = h(\Delta^c, \Delta^r) + o(1), \quad \rho \rightarrow \infty. \quad (96)$$

Then, using Theorem 2 and substituting (96) into (13), we obtain $C(\rho) \geq L^{(\xi)}(\rho)$, where

$$\begin{aligned} L^{(\xi)}(\rho) &= \log(2\pi) - (M-1)\log(e) - h(\Delta^c, \Delta^r) \\ &\quad + h(\underline{\mathbf{s}}^2) - \frac{1}{2}\mathbb{E}[\log(1+2\mathbf{s}_0^2)] - \frac{1}{2}\mathbb{E}[\log(1+2\mathbf{s}_1^2)] - \sum_{m=2}^{M-1} \mathbb{E}[g(m, \underline{\mathbf{s}})] + o(1). \end{aligned} \quad (97)$$

Next, we will characterize the high-SNR behavior of each term on the RHS of (97). Recall that $\underline{\mathbf{s}} \sim \mathcal{SG}_{\text{tr}}(\mu, \underline{\alpha}'(\gamma), \gamma)$ and that as $\rho \rightarrow \infty$, we have $\gamma \rightarrow 0$ and $\underline{\alpha}'(\gamma) \rightarrow \underline{\alpha}^*$. Thus, the pdf $f_{\underline{\mathbf{s}}}(t)$ converges to $f_{\underline{\tilde{\mathbf{s}}}}(t)$ for every t , where $\underline{\tilde{\mathbf{s}}} \sim \mathcal{SG}_{\text{tr}}(\mu, \underline{\alpha}^*, 0)$, and we obtain

$$\lim_{\gamma \rightarrow 0} h(\underline{\mathbf{s}}^2) = h(\underline{\tilde{\mathbf{s}}}^2), \quad (98)$$

$$\lim_{\gamma \rightarrow 0} \mathbb{E}[\log \mathbf{s}_m^2] = \mathbb{E}[\log \tilde{\mathbf{s}}_m^2]. \quad (99)$$

Using that $\log(1+a) = \log a + o(1)$ for all real $a > 1$, we can write

$$\mathbb{E}[\log(1+2\mathbf{s}_m^2)] = \mathbb{E}[\log \tilde{\mathbf{s}}_m^2] + \log 2 + o(1). \quad (100)$$

Moreover, since $\mathbb{E}[\log \tilde{\mathbf{s}}_m^2] = \log \mu + \psi(\alpha_m^*)$ [8] where $\psi(\cdot)$ is the Euler's digamma function, we can write

$$\begin{aligned} \mathbb{E}[\log \tilde{\mathbf{s}}_0^2] &= \log \mu + \psi\left(\frac{1}{2}\right), \\ \mathbb{E}[\log \tilde{\mathbf{s}}_1^2] &= \log \mu + \psi\left(\frac{1}{2}\right). \end{aligned} \quad (101)$$

Note that for all m , the elements $\tilde{\mathbf{s}}_m^2 \sim \mathcal{G}_{\text{tr}}(\mu, \alpha_m^*, 0)$ and independent of each other. Thus, the entropy of $\underline{\tilde{\mathbf{s}}}^2$ can be written as [31, Ch. 4.9]

$$\begin{aligned} h(\underline{\tilde{\mathbf{s}}}^2) &= \sum_{m=0}^{M-1} (\alpha_m^* \log e + \log \mu + \log \Gamma(\alpha_m^*) + (1-\alpha_m^*)\psi(\alpha_m^*)) \\ &\stackrel{(a)}{=} M \log \mu + \log(\pi) + (M-1)\log(e) + \psi\left(\frac{1}{2}\right), \end{aligned} \quad (102)$$

where (a) follows from the definition of $\underline{\alpha}^*$ in (10) and that $\sum_{m=0}^{M-1} \alpha_m^* = M-1$.

The following lemma helps to characterize the high-SNR behavior of the RHS of (97).

Lemma 25: For any deterministic vector $\underline{s} > \sqrt{\mu\gamma}$, we have

$$g(m, \underline{s}) = \begin{cases} \frac{1}{2} \log \left(1 + \frac{4s_2^2}{s_1^2} + \frac{s_2^2}{s_0^2} \right) + O \left(\frac{1}{\sqrt{\mu\gamma}} \right), & m = 2, \\ \frac{1}{2} \log \left(1 + \sum_{i=m-3}^{m-1} \frac{s_m^2}{s_i^2} \right) + O \left(\frac{1}{\sqrt{\mu\gamma}} \right), & m > 2, \end{cases} \quad (103)$$

Proof: See Appendix D.10. \square

Let $\tilde{\mathbf{u}} = \underline{s}/\sqrt{\mu}$, which leads to $\tilde{\mathbf{u}} \sim \mathcal{SG}_{\text{tr}}(1, \underline{\alpha}'(\gamma), \gamma)$. Then, using (103) and recalling that as $\rho \rightarrow \infty$, we have $\mu\gamma \rightarrow \infty$, $\gamma \rightarrow 0$, and $\underline{\alpha}'(\gamma) \rightarrow \underline{\alpha}^*$, we obtain

$$\begin{aligned} \lim_{\rho \rightarrow \infty} \mathbb{E}[g(m, \underline{s})] &= \lim_{\rho \rightarrow \infty} \mathbb{E}[g(m, \sqrt{\mu}\tilde{\mathbf{u}})] \\ &\stackrel{(a)}{=} g_{\text{hsnr}}(m), \end{aligned} \quad (104)$$

where $g_{\text{hsnr}}(\cdot)$ is defined in (19) and (a) follows because the pdf $f_{\tilde{\mathbf{u}}}(\underline{t})$ converges to $f_{\underline{\mathbf{u}}}(\underline{t})$ for every \underline{t} , where $\underline{\mathbf{u}} \sim \mathcal{SG}_{\text{tr}}(1, \underline{\alpha}^*, 0)$.

Finally, recalling $\mu = \rho/(M-1)$ and substituting (102) into (98), (101) into (100), and finally (98), (100), and (104) into (97) gives

$$L^{(\xi)}(\rho) = L_{\text{hsnr}}(\rho), \quad (105)$$

where $L_{\text{hsnr}}(\rho)$ is defined in (17), which completes the proof of Theorem 4.

APPENDIX D

PROOF OF LEMMAS NEEDED IN THEOREMS 1–4

This section is dedicated to the proof of lemmas used to prove Theorems 1–4. Before delving into the proofs, we define the following relations which will be used in some of the lemmas.

For all $m \in \{0, \dots, M-1\}$ and $k \in \{0, 1, \dots\}$, we define

$$\mathbf{z}_{k,m} = e^{-j(\boldsymbol{\theta}_{k,m} + \underline{\mathbf{X}}_{k,m})} \mathbf{w}_{k,m}, \quad (106)$$

which gives $\mathbf{z}_{k,m} \sim \mathcal{CN}(0, 1)$ and

$$\mathbf{s}_{k,m} = |\mathbf{x}_{k,m}|, \quad (107)$$

which results in rewriting (4) as

$$\mathbf{y}_{k,m} = e^{j(\boldsymbol{\theta}_{k,m} + \underline{\mathbf{X}}_{k,m})} (\mathbf{s}_{k,m} + \mathbf{z}_{k,m}). \quad (108)$$

Consequently, we have

$$|\mathbf{y}_{k,m}| = |\mathbf{s}_{k,m} + \mathbf{z}_{k,m}|, \quad (109)$$

$$\underline{\mathbf{y}}_{k,m} = \boldsymbol{\theta}_{k,m} \mp \underline{\mathbf{x}}_{k,m} \mp \underline{\mathbf{s}}_{k,m} + \underline{\mathbf{z}}_{k,m}. \quad (110)$$

The vector forms of the abovementioned parameters are defined as $\underline{\mathbf{z}}_k = \{\mathbf{z}_{k,m}\}_{m=0}^{M-1}$, $\underline{\mathbf{s}}_k = \{\mathbf{s}_{k,m}\}_{m=0}^{M-1}$, and $\underline{\mathbf{y}}_k = \{\mathbf{y}_{k,m}\}_{m=0}^{M-1}$.

In the following sections, the lemmas used in the proofs of Theorems 1–4 are presented. Specifically, Lemmas 16–18 are used for Theorem 1, Lemmas 19–22 for Theorem 2, Lemma 23 for Theorem 3, and Lemmas 25–24 for Theorem 4.

D.1 Proof of Lemma 16

Starting with the chain rule, we can write

$$I(\underline{\mathbf{x}}_1^n; \underline{\mathbf{y}}_1^n) = \sum_{k=1}^n I(\underline{\mathbf{x}}_1^n; \underline{\mathbf{y}}_k | \underline{\mathbf{y}}_1^{k-1}). \quad (111)$$

Following the footsteps of [8], we can upper-bound each term on the RHS of (111) as

$$\begin{aligned} I(\underline{\mathbf{x}}_1^n; \underline{\mathbf{y}}_k | \underline{\mathbf{y}}_1^{k-1}) &= h(\underline{\mathbf{y}}_k | \underline{\mathbf{y}}_1^{k-1}) - h(\underline{\mathbf{y}}_k | \underline{\mathbf{y}}_1^{k-1}, \underline{\mathbf{x}}_1^n) \\ &\stackrel{(a)}{\leq} h(\underline{\mathbf{y}}_k) - h(\underline{\mathbf{y}}_k | \underline{\mathbf{y}}_1^{k-1}, \underline{\mathbf{x}}_1^n) \\ &\stackrel{(b)}{=} h(\underline{\mathbf{y}}_k) - h(\underline{\mathbf{y}}_k | \underline{\mathbf{y}}_1^{k-1}, \underline{\mathbf{x}}_1^k) \\ &\stackrel{(c)}{\leq} h(\underline{\mathbf{y}}_k) - h(\underline{\mathbf{y}}_k | \underline{\mathbf{y}}_1^{k-1}, \underline{\mathbf{x}}_1^{k-1}, \underline{\mathbf{x}}_k, \boldsymbol{\theta}_{k-1}) \\ &\stackrel{(d)}{=} h(\underline{\mathbf{y}}_k) - h(\underline{\mathbf{y}}_k | \underline{\mathbf{x}}_k, \boldsymbol{\theta}_{k-1}) \\ &= I(\underline{\mathbf{y}}_k; \underline{\mathbf{x}}_k, \boldsymbol{\theta}_{k-1}) \\ &= I(\underline{\mathbf{x}}_k; \underline{\mathbf{y}}_k) + I(\underline{\mathbf{y}}_k; \boldsymbol{\theta}_{k-1} | \underline{\mathbf{x}}_k) \\ &\stackrel{(e)}{=} I(\underline{\mathbf{x}}_1; \underline{\mathbf{y}}_1) + I(\underline{\mathbf{y}}_1; \boldsymbol{\theta}_0 | \underline{\mathbf{x}}_1), \end{aligned} \quad (112)$$

where (a) and (c) follow as conditioning reduces entropy; (b) holds because based on (4)–(6), given $\underline{\mathbf{x}}_1^k$ the output $\underline{\mathbf{y}}_k$ is independent of future inputs $\underline{\mathbf{x}}_{k+1}^n$; (d) follows since given $\boldsymbol{\theta}_{k-1}$, the output $\underline{\mathbf{y}}_k$ is independent of the pair $(\underline{\mathbf{y}}_1^{k-1}, \underline{\mathbf{x}}_1^{k-1})$. Finally, (e) follows because $\{\underline{\mathbf{x}}_k\}$, $\{\underline{\mathbf{y}}_k\}$, and $\{\boldsymbol{\theta}_k\}$ are stationary processes.

Note that (112) holds for any channel in the form of (4)–(6) regardless of how the phase noises are correlated.

Finally, substituting (112) into (111), then (111) into (7) gives (69) and the proof is completed.

D.2 Proof of Lemma 17

By duality, for every probability distribution $\mathcal{Q}_{\underline{\mathbf{x}}_1}$ on $\underline{\mathbf{x}}_1$ and any pdf $f_{\underline{\mathbf{y}}_1}$ on $\underline{\mathbf{y}}_1$ we have [17]

$$I(\underline{\mathbf{x}}_1; \underline{\mathbf{y}}_1) \leq -\mathbb{E}[\log f_{\underline{\mathbf{y}}_1}(\underline{\mathbf{y}}_1)] - h(\underline{\mathbf{y}}_1 | \underline{\mathbf{x}}_1). \quad (113)$$

For any probability distribution $\mathcal{Q}_{\underline{\mathbf{x}}_1}$ satisfying $\mathbb{E}[\|\underline{\mathbf{x}}_1\|^2] \leq \rho$, we have

$$1 - \frac{\mathbb{E}[\|\underline{\mathbf{x}}_1\|^2] + M}{\rho + M} \geq 0. \quad (114)$$

Now for any given $\lambda \geq 0$,

$$I(\underline{\mathbf{x}}_1; \underline{\mathbf{y}}_1) \leq -\mathbb{E}[\log f_{\underline{\mathbf{y}}_1}(\underline{\mathbf{y}}_1)] - h(\underline{\mathbf{y}}_1 | \underline{\mathbf{x}}_1) + \lambda \left(1 - \frac{\mathbb{E}[\|\underline{\mathbf{x}}_1\|^2] + M}{\rho + M}\right). \quad (115)$$

To evaluate the first term on the RHS of (115), we take $\underline{\mathbf{y}}_1 \sim \mathcal{CSG}_{\text{tr}}(\mu, \underline{\alpha}, 0)$ and thus $f_{\underline{\mathbf{y}}_1}$ is defined according to (3), where we set $\mu = (\rho + M)/\alpha_{\Sigma}$ and $\alpha_{\Sigma} = \sum_{m=0}^{M-1} \alpha_m$. Essentially, we let each $\mathbf{y}_{1,m}$ be independent and circularly symmetric with the squared magnitude $|\mathbf{y}_{1,m}|^2$ following a single-variate gamma distribution.

Utilizing $f_{\underline{\mathbf{y}}_1}$ from (3) and that $\Gamma(\alpha, 0) = \Gamma(\alpha)$, the first term in the RHS of (115) can be evaluated as

$$\begin{aligned} -\mathbb{E}[\log f_{\underline{\mathbf{y}}_1}(\underline{\mathbf{y}}_1)] &= \alpha_{\Sigma} \log \frac{\rho + M}{\alpha_{\Sigma}} + \sum_{m=0}^{M-1} \log \Gamma(\alpha_m) + M \log \pi \\ &\quad + \sum_{m=0}^{M-1} (1 - \alpha_m) \mathbb{E}[\log |\mathbf{y}_{1,m}|^2] + \frac{\alpha_{\Sigma}}{\rho + M} \mathbb{E}[\|\underline{\mathbf{y}}_1\|^2] \cdot \log e. \end{aligned} \quad (116)$$

Note that $|\mathbf{y}_{1,m}| = |\mathbf{s}_{1,m} + \mathbf{z}_{1,m}|$ and $\mathbb{E}[\|\underline{\mathbf{y}}_1\|^2] = \mathbb{E}[\|\underline{\mathbf{s}}_1\|^2] + M$.

To lower bound the second term of the RHS of (115), we write the conditional differential entropy term as

$$\begin{aligned} h(\underline{\mathbf{y}}_1 | \underline{\mathbf{x}}_1) &= h(\mathbf{y}_{1,0} | \underline{\mathbf{x}}_1) + h(\mathbf{y}_{1,1} | \underline{\mathbf{x}}_1, \mathbf{y}_{1,0}) + \sum_{m=2}^{M-1} h(\mathbf{y}_{1,m} | \underline{\mathbf{x}}_1, \{\mathbf{y}_{1,i}\}_{i=0}^{m-1}) \\ &= h(\mathbf{y}_{1,0} | \mathbf{x}_{1,0}) + h(\mathbf{y}_{1,1} | \mathbf{x}_{1,0}, \mathbf{x}_{1,1}, \mathbf{y}_{1,0}) + \sum_{m=2}^{M-1} h(\mathbf{y}_m | \{\mathbf{x}_{1,i}\}_{i=0}^m, \{\mathbf{y}_{1,i}\}_{i=0}^{m-1}) \\ &\stackrel{(a)}{\geq} h(\mathbf{y}_{1,0} | \mathbf{x}_{1,0}) + h(\mathbf{y}_{1,1} | \mathbf{x}_{1,0}, \mathbf{x}_{1,1}, \mathbf{y}_{1,0}, \boldsymbol{\theta}_1^c) + \sum_{m=2}^{M-1} h(\mathbf{y}_{1,m} | \{\mathbf{x}_{1,i}\}_{i=0}^m, \{\mathbf{y}_{1,i}\}_{i=0}^{m-1}, \boldsymbol{\theta}_1^c, \boldsymbol{\theta}_1^r) \\ &\stackrel{(b)}{=} h(\mathbf{y}_{1,0} | \mathbf{x}_{1,0}) + h(\mathbf{y}_{1,1} | \mathbf{x}_{1,1}, \boldsymbol{\theta}_1^c) + (M-2) \log(\pi e), \end{aligned} \quad (117)$$

where (a) follows because conditioning reduces the entropy; (b) holds since when $\boldsymbol{\theta}_1^c$ is given, $\mathbf{y}_{1,1}$ is independent of the pair $(\mathbf{x}_{1,0}, \mathbf{y}_{1,0})$ and given the pair $(\boldsymbol{\theta}_1^c, \boldsymbol{\theta}_1^r)$, the last summation term becomes the summation of entropies of independent Gaussian variables, i.e., $(\mathbf{y}_{1,m} | \mathbf{x}_{1,m}, \boldsymbol{\theta}_1^c, \boldsymbol{\theta}_1^r) \sim \mathcal{CN}(e^{j(\boldsymbol{\theta}_1^c + m\boldsymbol{\theta}_1^r)} \mathbf{x}_{1,m}, 1)$.

Using (108), the first term on the RHS of (117) is

$$\begin{aligned}
h(\mathbf{y}_{1,0} | \mathbf{x}_{1,0}) &= h\left(e^{j(\theta_1^c + \underline{\mathbf{L}}\mathbf{x}_{1,0})}(\mathbf{s}_{1,0} + \mathbf{z}_{1,0}) | \mathbf{s}_{1,0}, \underline{\mathbf{L}}\mathbf{x}_{1,0}\right) \\
&\stackrel{(a)}{=} h\left(e^{j\theta_1^c}(\mathbf{s}_{1,0} + \mathbf{z}_{1,0}) | \mathbf{s}_{1,0}\right) \\
&\stackrel{(b)}{=} h(|\mathbf{s}_{1,0} + \mathbf{z}_{1,0}|^2 | \mathbf{s}_{1,0}) + \log \pi,
\end{aligned} \tag{118}$$

where (a) follows because $\mathbf{z}_{1,0}$ defined in (106) is circularly symmetric and its distribution remains the same with rotation; to obtain (b) we applied Lemma 5 as $e^{j\theta_1^c}(\mathbf{s}_{1,0} + \mathbf{z}_{1,0})$ is circularly symmetric given $\mathbf{s}_{1,0}$. Following the same steps leading to (118), the second term on RHS of (117) can be written as

$$\begin{aligned}
h(\mathbf{y}_{1,1} | \mathbf{x}_{1,1}, \theta_1^c) &= h\left(e^{j(\theta_1^c + \theta_1^r)}(\mathbf{s}_{1,1} + \mathbf{z}_{1,1}) | \mathbf{s}_{1,1}, \theta_1^c\right) \\
&= h(|\mathbf{s}_{1,1} + \mathbf{z}_{1,1}|^2 | \mathbf{s}_{1,1}) + \log \pi.
\end{aligned} \tag{119}$$

Combining (119) and (118) into (117) gives

$$h(\underline{\mathbf{y}}_1 | \underline{\mathbf{x}}_1) \geq h(|\mathbf{s}_{1,0} + \mathbf{z}_{1,0}|^2 | \mathbf{s}_{1,0}) + h(|\mathbf{s}_{1,1} + \mathbf{z}_{1,1}|^2 | \mathbf{s}_{1,1}) + \log(\pi^M) + (M - 2) \log e. \tag{120}$$

Substituting (116) and (120) into (115) gives

$$\begin{aligned}
I(\underline{\mathbf{x}}_1; \underline{\mathbf{y}}_1) &\leq \alpha_\Sigma \log \frac{\rho + M}{\alpha_\Sigma} + \lambda - (M - 2) \log e \\
&\quad + \sum_{m=0}^{M-1} (\log \Gamma(\alpha_m) + (1 - \alpha_m) \mathbb{E} [\log (|\mathbf{s}_{1,m} + \mathbf{z}_{1,m}|^2)]) \\
&\quad + (\alpha_\Sigma \log e - \lambda) \left(\frac{\mathbb{E}[\|\underline{\mathbf{s}}_1\|^2] + M}{\rho + M} \right) \\
&\quad - h(|\mathbf{s}_{1,0} + \mathbf{z}_{1,0}|^2 | \mathbf{s}_{1,0}) - h(|\mathbf{s}_{1,1} + \mathbf{z}_{1,1}|^2 | \mathbf{s}_{1,1}) \\
&= \alpha_\Sigma \log \left(\frac{\rho + M}{\alpha_\Sigma} \right) + d_{\lambda, \alpha} + R_{\lambda, \alpha}(\rho, \underline{\mathbf{s}}_1),
\end{aligned} \tag{121}$$

where $R_{\lambda, \alpha}(\cdot)$ and $d_{\lambda, \alpha}$ are defined in (11) and (71), respectively.

Finally, replacing back $\underline{\mathbf{s}}_1$ with $|\underline{\mathbf{x}}_1|$ gives (70) and completes the proof.

D.3 Proof of Lemma 18

The proof is divided into two parts. The first part simplifies the RHS (69) for $M = 2$, and the second part provides an upper bound on the RHS of (69) for $M > 2$.

The second term on the RHS of (69) for $M = 2$:

From (106)–(108) we can write $\underline{y}_1 = \underline{\theta}_1 \mp \underline{x}_1 \mp \underline{s}_1 + \underline{z}_1$. Then, applying the chain rule on the second term on the RHS of (69) gives

$$\begin{aligned}
I(\underline{y}_1; \underline{\theta}_0 \mid \underline{x}_1) &\stackrel{(a)}{=} I(\underline{y}_1; \underline{\theta}_0 \mid \underline{x}_1, |\underline{y}_1|) \\
&= I(\underline{y}_1 \mp \underline{x}_1; \underline{\theta}_0 \mid \underline{x}_1, |\underline{y}_1|) \\
&\stackrel{(b)}{=} I(\underline{\theta}_1 \mp \underline{s}_1 + \underline{z}_1; \underline{\theta}_0 \mid \underline{s}_1, |\underline{y}_1|) \\
&= h(\underline{\theta}_1 \mp \underline{s}_1 + \underline{z}_1 \mid \underline{s}_1, |\underline{y}_1|) - h(\underline{\theta}_1 \mp \underline{s}_1 + \underline{z}_1 \mid \underline{s}_1, |\underline{y}_1|, \underline{\theta}_0) \\
&\stackrel{(c)}{=} 2 \log(2\pi) - h(\underline{\theta}_1 \mp \underline{s}_1 + \underline{z}_1 \mid \underline{s}_1, |\underline{y}_1|, \underline{\theta}_0) \\
&= 2 \log(2\pi) - h(\{\theta_1^c \mp m\theta_1^r \mp \underline{s}_{1,m} + \underline{z}_{1,m}\}_0^1 \mid \underline{s}_1, |\underline{s}_1 + \underline{z}_1|, \underline{\theta}_0) \\
&= 2 \log(2\pi) - h(\{\Delta_1^c \mp m\Delta_1^r \mp \underline{s}_{1,m} + \underline{z}_{1,m}\}_0^1 \mid \underline{s}_1, |\underline{s}_1 + \underline{z}_1|)
\end{aligned} \tag{122}$$

where (a) holds since the pair $(|\underline{y}_1|, \underline{\theta}_0)$ are independent; (b) follows since $\underline{s}_1 = |\underline{x}_1|$ and \underline{x}_1 are independent as \underline{x}_1 is circularly symmetric; (c) holds since the two components of $\underline{\theta}_1 = (\theta_1^c, \theta_1^r \mp \theta_1^r)$ are independent and uniform on $[-\pi, \pi)$, from which follows that the components of $\underline{\theta}_1 \mp \underline{s}_1 + \underline{z}_1$ are also independent and uniform on $[-\pi, \pi)$.

The second term on the RHS of (69) for $M > 2$:

$$\begin{aligned}
I(\underline{y}_1; \underline{\theta}_0 \mid \underline{x}_1) &\leq I(\underline{y}_1, \theta_1^r; \underline{\theta}_0 \mid \underline{x}_1) \\
&= I(\theta_1^r; \underline{\theta}_0 \mid \underline{x}_1) + I(\underline{y}_1; \underline{\theta}_0 \mid \underline{x}_1, \theta_1^r) \\
&\stackrel{(a)}{=} I(\theta_1^r; \theta_0^c, \theta_0^r \mid \underline{x}_1) + I(\underline{y}_1; \theta_0^c, \theta_0^r \mid \underline{x}_1, \theta_1^r) \\
&\stackrel{(b)}{=} I(\theta_1^r; \theta_0^r \mid \underline{x}_1) + I(\underline{y}_1; \theta_0^c \mid \underline{x}_1, \theta_1^r),
\end{aligned} \tag{123}$$

where (a) holds since (θ_0^c, θ_0^r) are sufficient statistics for $\underline{\theta}_0$, and (b) follows because, given θ_1^r , the pair $(\underline{y}_1, \theta_0^r)$ is independent, hence $I(\underline{y}_1; \theta_0^r \mid \underline{x}_1, \theta_1^r) = 0$.

The first term on the RHS of (123) is

$$\begin{aligned}
I(\theta_1^r; \theta_0^r \mid \underline{x}_1) &\stackrel{(a)}{=} I(\theta_1^r; \theta_0^r) \\
&= h(\theta_1^r) - h(\theta_1^r \mid \theta_0^r) \\
&= \log(2\pi) - h(\Delta_1^r),
\end{aligned} \tag{124}$$

where (a) holds since (θ_1^r, θ_0^r) are independent of the inputs \underline{x}_1 .

Recall $\mathbf{y}_{1,m}$ and $\mathbf{z}_{1,m}$ from (108) and (106), respectively. Then, define

$$\begin{aligned}\tilde{\mathbf{y}}_{1,m} &= e^{-jm\boldsymbol{\theta}_1^r} \mathbf{y}_{1,m} \\ &= e^{j\boldsymbol{\theta}_1^c + \angle \mathbf{x}_{1,m}} (\mathbf{s}_{1,m} + \mathbf{z}_{1,m}),\end{aligned}\quad (125)$$

and its vector form as $\tilde{\mathbf{y}}_{\underline{1}} = (\tilde{\mathbf{y}}_{1,0}, \dots, \tilde{\mathbf{y}}_{1,M-1})$. Then, the second term on the RHS of (123) can be written as

$$\begin{aligned}I(\underline{\mathbf{y}}_{\underline{1}}; \boldsymbol{\theta}_0^c \mid \underline{\mathbf{x}}_{\underline{1}}, \boldsymbol{\theta}_1^r) &= I\left(\left\{e^{-jm\boldsymbol{\theta}_1^r} \mathbf{y}_{1,m}\right\}_{m=0}^{M-1}; \boldsymbol{\theta}_0^c \mid \underline{\mathbf{x}}_{\underline{1}}, \boldsymbol{\theta}_1^r\right) \\ &\stackrel{(a)}{=} I(\tilde{\mathbf{y}}_{\underline{1}}; \boldsymbol{\theta}_0^c \mid \underline{\mathbf{x}}_{\underline{1}}),\end{aligned}\quad (126)$$

where in (a) we used that $\tilde{\mathbf{y}}_{\underline{1}}$ is independent of $\boldsymbol{\theta}_1^r$.

Recall $\|\underline{\mathbf{x}}_{\underline{1}}\| = \|\underline{\mathbf{s}}_{\underline{1}}\|$ and define $\underline{\mathbf{u}}_{\underline{1}} = \underline{\mathbf{x}}_{\underline{1}} / \|\underline{\mathbf{x}}_{\underline{1}}\| = \exp(j\angle \underline{\mathbf{x}}_{\underline{1}}) \circ \underline{\mathbf{s}}_{\underline{1}} / \|\underline{\mathbf{s}}_{\underline{1}}\|$. Let the matrix $\mathbf{U} = (\underline{\mathbf{u}}_{\underline{1}}^T, \underline{\mathbf{u}}_{\underline{2}}^T, \dots, \underline{\mathbf{u}}_{\underline{M}}^T)^T$ with $\underline{\mathbf{u}}_{\underline{2}}, \dots, \underline{\mathbf{u}}_{\underline{M}}$ are vectors orthogonal to $\underline{\mathbf{u}}_{\underline{1}}^\dagger$ and mutually orthonormal i.e., $\mathbf{U}^\dagger \mathbf{U} = I_M$. Then RHS of (126) can be written as

$$\begin{aligned}I(\tilde{\mathbf{y}}_{\underline{1}}; \boldsymbol{\theta}_0^c \mid \underline{\mathbf{x}}_{\underline{1}}) &= I(\mathbf{U}^\dagger \tilde{\mathbf{y}}_{\underline{1}}; \boldsymbol{\theta}_0^c \mid \mathbf{U}^\dagger \underline{\mathbf{x}}_{\underline{1}}) \\ &\stackrel{(a)}{=} I(\underline{\mathbf{u}}_{\underline{1}}^\dagger \tilde{\mathbf{y}}_{\underline{1}}; \boldsymbol{\theta}_0^c \mid \underline{\mathbf{u}}_{\underline{1}}^\dagger \underline{\mathbf{x}}_{\underline{1}}) \\ &\stackrel{(b)}{=} I(e^{j\boldsymbol{\theta}_1^c} (\|\underline{\mathbf{s}}_{\underline{1}}\| + \mathbf{v}_1); \boldsymbol{\theta}_0^c \mid \|\underline{\mathbf{s}}_{\underline{1}}\|) \\ &\stackrel{(c)}{=} I(\boldsymbol{\theta}_1^c \mp \angle \|\underline{\mathbf{s}}_{\underline{1}}\| + \mathbf{v}_1; \boldsymbol{\theta}_0^c \mid \|\underline{\mathbf{s}}_{\underline{1}}\|, \|\|\underline{\mathbf{s}}_{\underline{1}}\| + \mathbf{v}_1\|) \\ &\stackrel{(d)}{=} \log(2\pi) - h(\boldsymbol{\Delta}_1^c \mp \angle \|\underline{\mathbf{s}}_{\underline{1}}\| + \mathbf{v}_1 \mid \|\underline{\mathbf{s}}_{\underline{1}}\|, \|\|\underline{\mathbf{s}}_{\underline{1}}\| + \mathbf{v}_1\|).\end{aligned}\quad (127)$$

Here, (a) holds since $\underline{\mathbf{u}}_{\underline{1}}^\dagger \tilde{\mathbf{y}}_{\underline{1}}$ is sufficient statistics for $\boldsymbol{\theta}_0^c$ as $\underline{\mathbf{u}}_{\underline{1}}^\dagger \tilde{\mathbf{y}}_{\underline{1}} \sim \mathcal{CN}(0, 1)$ and independent of $\boldsymbol{\theta}_0^c$ for all $i \in \{2, \dots, M\}$; in (b) $\mathbf{v}_1 = \underline{\mathbf{u}}_{\underline{1}}^\dagger \mathbf{z}_{\underline{1}}$ resulting in $\mathbf{v}_1 \sim \mathcal{CN}(0, 1)$; in (c) the pair $(\boldsymbol{\theta}_0^c, \|\|\underline{\mathbf{s}}_{\underline{1}}\| + \mathbf{v}_1\|)$ are independent; finally, (d) holds since $\boldsymbol{\theta}_1^c \sim \mathcal{U}[-\pi, \pi)$. Substituting (124), (126) and then (127) into (123) we have

$$I(\underline{\mathbf{y}}_{\underline{1}}; \boldsymbol{\theta}_0 \mid \underline{\mathbf{x}}_{\underline{1}}) \leq 2 \log(2\pi) - h(\boldsymbol{\Delta}_1^r) - h(\boldsymbol{\Delta}_1^c \mp \angle \|\underline{\mathbf{s}}_{\underline{1}}\| + \mathbf{v}_1 \mid \|\underline{\mathbf{s}}_{\underline{1}}\|, \|\|\underline{\mathbf{s}}_{\underline{1}}\| + \mathbf{v}_1\|). \quad (128)$$

Now, replacing $\underline{\mathbf{s}}_{\underline{1}}$ with $|\underline{\mathbf{x}}_{\underline{1}}|$ and combining (128) and (122) gives

$$I(\underline{\mathbf{y}}_{\underline{1}}; \boldsymbol{\theta}_0 \mid \underline{\mathbf{x}}_{\underline{1}}) \leq 2 \log(2\pi) + F(M, |\underline{\mathbf{x}}_{\underline{1}}|, \boldsymbol{\Delta}_1^c, \boldsymbol{\Delta}_1^r), \quad (129)$$

where $F(\cdot)$ is defined in (12).

D.4 Proof of Lemma 19

To initiate the derivation of the lower bound, we apply the chain rule, leveraging the non-negativity of mutual information. This allows us to write

$$\begin{aligned} I(\underline{\mathbf{x}}_1^n; \underline{\mathbf{y}}_1^n) &= \sum_{k=1}^n I(\underline{\mathbf{x}}_k; \underline{\mathbf{y}}_1^n | \underline{\mathbf{x}}_1^{k-1}) \\ &\geq \sum_{k=2}^n I(\underline{\mathbf{x}}_k; \underline{\mathbf{y}}_1^k | \underline{\mathbf{x}}_1^{k-1}). \end{aligned} \quad (130)$$

Fix $k \geq 2$ and set

$$\epsilon_k = I(\underline{\mathbf{x}}_k; \underline{\boldsymbol{\theta}}_{k-1} | \underline{\mathbf{x}}_{k-1}, \underline{\mathbf{y}}_{k-1}, \underline{\mathbf{y}}_k). \quad (131)$$

Following similar footsteps as in [8], we can write

$$\begin{aligned} I(\underline{\mathbf{x}}_k; \underline{\mathbf{y}}_1^k | \underline{\mathbf{x}}_1^{k-1}) &\stackrel{(a)}{=} I(\underline{\mathbf{x}}_k; \underline{\mathbf{y}}_1^k, \underline{\mathbf{x}}_1^{k-1}) \\ &\stackrel{(b)}{\geq} I(\underline{\mathbf{x}}_k; \underline{\mathbf{y}}_k, \underline{\mathbf{y}}_{k-1}, \underline{\mathbf{x}}_{k-1}) \\ &= I(\underline{\mathbf{x}}_k; \underline{\mathbf{y}}_k, \underline{\mathbf{y}}_{k-1}, \underline{\mathbf{x}}_{k-1}, \underline{\boldsymbol{\theta}}_{k-1}) - \epsilon_k \\ &\stackrel{(c)}{=} I(\underline{\mathbf{x}}_k; \underline{\mathbf{y}}_k, \underline{\boldsymbol{\theta}}_{k-1}) - \epsilon_k \\ &\stackrel{(d)}{=} I(\underline{\mathbf{x}}_k; \underline{\mathbf{y}}_k | \underline{\boldsymbol{\theta}}_{k-1}) - \epsilon_k \\ &\stackrel{(e)}{=} I(\underline{\mathbf{x}}_2; \underline{\mathbf{y}}_2 | \underline{\boldsymbol{\theta}}_1) - \epsilon_2, \end{aligned} \quad (132)$$

where (a) holds since $\{\underline{\mathbf{x}}_k\}$ are independent; (b) is a consequence of the chain rule and nonnegativity of mutual information; (c) follows because when the pair $(\underline{\boldsymbol{\theta}}_{k-1}, \underline{\mathbf{y}}_k)$ is given, $\underline{\mathbf{x}}_k$ and the pair $(\underline{\mathbf{y}}_{k-1}, \underline{\mathbf{x}}_{k-1})$ are conditionally independent; (d) follows because $\underline{\mathbf{x}}_k$ and $\underline{\boldsymbol{\theta}}_{k-1}$ are independent; finally (e) holds due to stationarity. Substituting (132) into (130) and the result into (7) gives (75) for all distributions on $\underline{\mathbf{x}}_2$ such that $\mathbb{E}[\|\underline{\mathbf{x}}_2\|] \leq \rho$.

D.5 Proof of Lemma 20

The first term on the RHS of (79) can be written as

$$h(\{\mathbf{y}_{2,m}\}_0^1 | \underline{\mathbf{x}}_2, \underline{\boldsymbol{\theta}}_1) \stackrel{(a)}{=} h(\{\|\mathbf{y}_{2,m}\|^2\}_0^1 | \underline{\mathbf{x}}_2, \underline{\boldsymbol{\theta}}_1) - 2 \log 2 + h(\{\underline{\mathbf{y}}_{2,m}\}_0^1 | \underline{\mathbf{x}}_2, \underline{\boldsymbol{\theta}}_1, \{\|\mathbf{y}_{2,m}\}\}_0^1), \quad (133)$$

where (a) follows by utilizing Lemma 5. We continue by upper-bounding each entropy term in (133).

The first term can be upper-bounded as

$$\begin{aligned} h(\{\|\mathbf{y}_{2,m}\|^2\}_0^1 | \underline{\mathbf{x}}_2, \underline{\boldsymbol{\theta}}_1) &\stackrel{(a)}{=} h(\{\|\mathbf{y}_{2,m}\|^2\}_0^1 | \underline{\mathbf{x}}_2, \underline{\boldsymbol{\theta}}_1) \\ &\stackrel{(b)}{=} h(\|\mathbf{y}_{2,0}\|^2 | \|\mathbf{x}_{2,0}\|) + h(\|\mathbf{y}_{2,1}\|^2 | \|\mathbf{x}_{2,1}\|) \\ &\stackrel{(c)}{\leq} \log(2\pi e) + \frac{1}{2} \mathbb{E} \left[\log \left(1 + 2 \|\mathbf{x}_{2,0}\|^2 \right) \right] + \frac{1}{2} \mathbb{E} \left[\log \left(1 + 2 \|\mathbf{x}_{2,1}\|^2 \right) \right], \end{aligned} \quad (134)$$

where (a) holds since $\mathbf{y}_{2,m}$ are independent of $\underline{\mathbf{x}}_2$. Moreover, (b) follows as $|\mathbf{y}_{2,0}|$ and $|\mathbf{y}_{2,1}|$ in (109) are independent of $\underline{\boldsymbol{\theta}}_1$ and each other; the inequality in (c) is obtained by recalling (109) and applying Lemma 7 on both entropy terms.

The second term on the RHS of (133) can be upper-bounded as

$$\begin{aligned} h\left(\{\underline{\mathbf{y}}_{2,m}\}_0^1 \mid \underline{\mathbf{x}}_2, \underline{\boldsymbol{\theta}}_1, \{|\mathbf{y}_{2,m}|\}_0^1\right) &= h\left(\{\underline{\mathbf{y}}_{2,m} \stackrel{\pi}{-} \underline{\mathbf{x}}_{2,m} \stackrel{\pi}{-} \boldsymbol{\theta}_{1,m}\}_0^1 \mid \underline{\mathbf{x}}_2, \underline{\boldsymbol{\theta}}_1, \{|\mathbf{y}_{2,m}|\}_0^1\right) \\ &\stackrel{(a)}{=} h\left(\{\Delta_2^c \stackrel{\mp}{+} m\Delta_2^r \stackrel{\mp}{+} \underline{|\mathbf{x}_{2,m}|} + \mathbf{z}_{2,m}\}_0^1 \mid \underline{\mathbf{x}}_2, \{|\mathbf{y}_{2,m}|\}_0^1\right), \end{aligned} \quad (135)$$

where in (a) we used from (110) that $\underline{\mathbf{y}}_{2,m} = \boldsymbol{\theta}_{2,m} \stackrel{\mp}{+} \underline{\mathbf{x}}_{2,m} \stackrel{\mp}{+} \underline{|\mathbf{x}_{2,m}|} + \mathbf{z}_{2,m}$ and that $\boldsymbol{\theta}_{2,m} \stackrel{\pi}{-} \boldsymbol{\theta}_{1,m} = \Delta_2^c \stackrel{\mp}{+} m\Delta_2^r$. Note that the elements of $\underline{\mathbf{x}}_2$ are irrelevant to the entropy. Hence, they are omitted from the conditions.

This concludes the proof.

D.6 Proof of Lemma 21

We can characterize the second term on the RHS of (79) as follows

$$\begin{aligned} &h\left(\{\mathbf{y}_{2,m}\}_2^{M-1} \mid \underline{\mathbf{x}}_2, \{\mathbf{y}_{2,m}\}_0^1\right) \\ &= \sum_{m=2}^{M-1} h\left(\mathbf{y}_{2,m} \mid \underline{\mathbf{x}}_2, \{\mathbf{y}_{2,i}\}_{i=0}^{m-1}\right) \\ &\stackrel{(a)}{=} \sum_{m=2}^{M-1} I\left(\mathbf{y}_{2,m}; \underline{\boldsymbol{\theta}}_2 \mid \underline{\mathbf{x}}_2, \{\mathbf{y}_{2,i}\}_{i=0}^{m-1}\right) + h\left(\mathbf{y}_{2,m} \mid \underline{\mathbf{x}}_2, \underline{\boldsymbol{\theta}}_2, \{\mathbf{y}_{2,i}\}_{i=0}^{m-1}\right) \\ &\stackrel{(b)}{=} (M-2)\log(\pi e) + \sum_{m=2}^{M-1} I\left(\underline{\mathbf{y}}_{2,m}; \underline{\boldsymbol{\theta}}_2 \mid \underline{\mathbf{x}}_2, \{\underline{\mathbf{y}}_{2,i}\}_{i=0}^{m-1}, \{|\mathbf{y}_{2,i}|\}_{i=0}^m\right) \\ &= (M-2)\log(\pi e) \\ &\quad + \sum_{m=2}^{M-1} \left(h\left(\underline{\mathbf{y}}_{2,m} \mid \underline{\mathbf{x}}_2, \{\underline{\mathbf{y}}_{2,i}\}_{i=0}^{m-1}, \{|\mathbf{y}_{2,i}|\}_{i=0}^m\right) - h\left(\underline{\mathbf{y}}_{2,m} \mid \underline{\mathbf{x}}_2, \underline{\boldsymbol{\theta}}_2, \{\underline{\mathbf{y}}_{2,i}\}_{i=0}^{m-1}, \{|\mathbf{y}_{2,i}|\}_{i=0}^m\right) \right) \end{aligned} \quad (136)$$

where (a) follows from the definition of mutual information and (b) holds since it is evident from (108)–(109) that $|\mathbf{y}_{2,m}|$ and $\underline{\boldsymbol{\theta}}_2$ are independent, and $(\mathbf{y}_{2,m} \mid \underline{\mathbf{x}}_{2,m}, \underline{\boldsymbol{\theta}}_2) \sim \mathcal{CN}(e^{j\boldsymbol{\theta}_{2,m}} \mathbf{x}_{2,m}, 1)$ for all $m \in \{2, \dots, M-1\}$.

Next, we upper-bound each entropy term in the first summation term on the RHS of (136). We consider the cases of $m = 2$ and $m > 2$ separately.

We first define

$$\mathbf{y}'_{k,m} = e^{-j\underline{\mathbf{x}}_{k,m}} \mathbf{y}_{k,m}, \quad (137)$$

which implies

$$\begin{aligned} \underline{\mathbf{y}}'_{k,m} &= \underline{\mathbf{y}}_{k,m} \stackrel{\pi}{-} \underline{\mathbf{x}}_{k,m} \\ &= \boldsymbol{\theta}_{k,m} \stackrel{\mp}{+} \underline{\mathbf{s}}_{k,m} + \mathbf{z}_{k,m}. \end{aligned} \quad (138)$$

Then, starting with the case $m = 2$, we obtain

$$\begin{aligned} &h\left(\underline{\mathbf{y}}_{2,2} \mid \underline{\mathbf{x}}_2, \{\underline{\mathbf{y}}_{2,i}\}_{i=0}^1, \{|\mathbf{y}_{2,i}|\}_{i=0}^2\right) \\ &= h\left(\underline{\mathbf{y}}_{2,2} \stackrel{\pi}{-} \underline{\mathbf{x}}_{2,2} \mid \underline{\mathbf{x}}_2, |\underline{\mathbf{x}}_2|, \{\underline{\mathbf{y}}_{2,i}\}_{i=0}^1, \{|\mathbf{y}_{2,i}|\}_{i=0}^2\right) \\ &\stackrel{(a)}{=} h\left(\underline{\mathbf{y}}'_{2,2} \mid |\underline{\mathbf{x}}_2|, \{\underline{\mathbf{y}}'_{2,i}\}_{i=0}^1, \{|\mathbf{y}_{2,i}|\}_{i=0}^2\right) \\ &\stackrel{(b)}{=} h\left(\underline{\mathbf{y}}'_{2,2} \stackrel{\pi}{-} 2\underline{\mathbf{y}}'_{2,1} \stackrel{\mp}{+} \underline{\mathbf{y}}'_{2,0} \mid |\underline{\mathbf{x}}_2|, \{\underline{\mathbf{y}}'_{2,i}\}_{i=0}^1, \{|\mathbf{y}_{2,i}|\}_{i=0}^2\right) \\ &\stackrel{(c)}{\leq} h\left(\underline{\mathbf{y}}'_{2,2} \stackrel{\pi}{-} 2\underline{\mathbf{y}}'_{2,1} \stackrel{\mp}{+} \underline{\mathbf{y}}'_{2,0} \mid |\underline{\mathbf{x}}_2|, \{|\mathbf{y}_{2,i}|\}_{i=0}^2\right) \\ &\stackrel{(d)}{=} h\left(\underline{|\mathbf{x}_{2,2}| + \mathbf{z}_{2,2}} \stackrel{\pi}{-} 2\underline{|\mathbf{x}_{2,1}| + \mathbf{z}_{2,1}} \stackrel{\mp}{+} \underline{|\mathbf{x}_{2,0}| + \mathbf{z}_{2,0}} \mid |\underline{\mathbf{x}}_2|, \{|\mathbf{y}_{2,i}|\}_{i=0}^2\right) \\ &\stackrel{(e)}{=} h\left(\phi(2, |\underline{\mathbf{x}}_2|) \mid |\underline{\mathbf{x}}_2|, \{|\mathbf{y}_{2,i}|\}_{i=0}^2\right), \end{aligned} \quad (139)$$

where (a) follows directly from (138) and that $\underline{\mathbf{x}}_2$ is irrelevant for $\underline{\mathbf{y}}'_{2,2}$, (b) follows as we added or subtracted given phases which does not change the entropy, and (c) holds as conditioning reduces the entropy. Moreover, in (d) we used that according to (5) for $m = 2$ we have $\boldsymbol{\theta}_{2,2} = 2\boldsymbol{\theta}_{2,1} \stackrel{\pi}{-} \boldsymbol{\theta}_{2,0}$; finally, in (e) the $\phi(\cdot)$ function is defined in (15).

For the case $m > 2$, we follow similar footsteps as in (139) and write

$$\begin{aligned} &h\left(\underline{\mathbf{y}}_{2,m} \mid \underline{\mathbf{x}}_2, \{\underline{\mathbf{y}}_{2,i}\}_{i=0}^{m-1}, \{|\mathbf{y}_{2,i}|\}_{i=0}^m\right) \\ &= h\left(\underline{\mathbf{y}}'_{2,m} \mid |\underline{\mathbf{x}}_2|, \{\underline{\mathbf{y}}'_{2,i}\}_{i=0}^{m-1}, \{|\mathbf{y}_{2,i}|\}_{i=0}^m\right) \\ &= h\left(\underline{\mathbf{y}}'_{2,m} \stackrel{\pi}{-} \underline{\mathbf{y}}'_{2,m-1} \stackrel{\pi}{-} \underline{\mathbf{y}}'_{2,m-2} \stackrel{\mp}{+} \underline{\mathbf{y}}'_{2,m-3} \mid |\underline{\mathbf{x}}_2|, \{\underline{\mathbf{y}}'_{2,i}\}_{i=0}^{m-1}, \{|\mathbf{y}_{2,i}|\}_{i=0}^m\right) \\ &\stackrel{(a)}{\leq} h\left(\phi(m, |\underline{\mathbf{x}}_2|) \mid |\underline{\mathbf{x}}_2|, \{|\mathbf{y}_{2,i}|\}_{i=0}^m\right), \end{aligned} \quad (140)$$

where in the last inequality, we used that the conditioning reduces entropy and that $\boldsymbol{\theta}_{2,m} = \boldsymbol{\theta}_{2,m-1} \stackrel{\mp}{+} \boldsymbol{\theta}_{2,m-2} \stackrel{\pi}{-} \boldsymbol{\theta}_{2,m-3}$, for $m > 2$. Note that we could possibly use $\boldsymbol{\theta}_{2,m} = 2\boldsymbol{\theta}_{2,m-1} \stackrel{\pi}{-} \boldsymbol{\theta}_{2,m-2}$ as in (139) but it would lead to a looser bound. Finally, combining (139) and (140) we obtain for $m \geq 2$

$$h\left(\underline{\mathbf{y}}_{2,m} \mid \underline{\mathbf{x}}_2, \{\underline{\mathbf{y}}_{2,i}\}_{i=0}^{m-1}, \{|\mathbf{y}_{2,i}|\}_{i=0}^m\right) \leq h\left(\phi(m, |\underline{\mathbf{x}}_2|) \mid |\underline{\mathbf{x}}_2|, \{|\mathbf{y}_{2,i}|\}_{i=0}^m\right). \quad (141)$$

For the second entropy term on the RHS of (136),

$$\begin{aligned}
h\left(\underline{\mathbf{y}}_{2,m} \mid \underline{\mathbf{x}}_2, \underline{\boldsymbol{\theta}}_2, \{\underline{\mathbf{y}}_{2,i}\}_{i=0}^{m-1}, \{|\mathbf{y}_{2,i}|\}_{i=0}^m\right) &= h\left(\underline{\mathbf{y}}_{2,m} - \underline{\mathbf{x}}_{2,m} \mid \underline{\mathbf{x}}_2, \underline{\boldsymbol{\theta}}_2, \{\underline{\mathbf{y}}_{2,i}\}_{i=0}^{m-1}, \{|\mathbf{y}_{2,i}|\}_{i=0}^m\right) \\
&\stackrel{(a)}{=} h\left(\underline{\boldsymbol{\theta}}_{2,m} \mp \underline{\mathbf{x}}_{2,m} \mid \underline{\mathbf{x}}_{2,m}, \underline{\boldsymbol{\theta}}_{2,m}, |\mathbf{y}_{2,m}|\right) \\
&\stackrel{(b)}{=} h\left(\underline{\mathbf{x}}_{2,m} \mid \underline{\mathbf{x}}_{2,m}, |\mathbf{y}_{2,m}|\right), \tag{142}
\end{aligned}$$

where (a) follows as $\{\underline{\mathbf{y}}_{2,i}\}_{i=0}^{m-1}$ are irrelevant given $\underline{\boldsymbol{\theta}}_{2,m}$ and (b) follows since $\underline{\boldsymbol{\theta}}_{2,m}$ is independent of $\underline{\mathbf{x}}_{2,m}$.

Substituting (141) and (142) into (136) gives

$$\begin{aligned}
&h\left(\{\mathbf{y}_{2,m}\}_{m=2}^{M-1} \mid \underline{\mathbf{x}}_2, \mathbf{y}_{2,0}, \mathbf{y}_{2,1}\right) \\
&\leq (M-2) \log(\pi e) + \sum_{m=2}^{M-1} \left(h\left(\phi(m, \underline{\mathbf{x}}_2) \mid \underline{\mathbf{x}}_2, \{|\mathbf{y}_{2,i}|\}_{i=0}^m\right) - h\left(\underline{\mathbf{x}}_{2,m} \mid \underline{\mathbf{x}}_{2,m}, |\mathbf{y}_{2,m}|\right) \right) \\
&= (M-2) \log(\pi e) + \sum_{m=2}^{M-1} \mathbb{E}[g(m, \underline{\mathbf{x}}_2)], \tag{143}
\end{aligned}$$

where $g(\cdot)$ is defined in (14). This concludes the proof.

D.7 Proof of Lemma 22

Following similar steps as in [17, App. IX], we can write

$$\begin{aligned}
I(\underline{\mathbf{x}}_2; \underline{\boldsymbol{\theta}}_1 \mid \underline{\mathbf{x}}_1, \underline{\mathbf{y}}_1, \underline{\mathbf{y}}_2) &= h(\underline{\boldsymbol{\theta}}_1 \mid \underline{\mathbf{x}}_1, \underline{\mathbf{y}}_1, \underline{\mathbf{y}}_2) - h(\underline{\boldsymbol{\theta}}_1 \mid \underline{\mathbf{x}}_1, \underline{\mathbf{x}}_2, \underline{\mathbf{y}}_1, \underline{\mathbf{y}}_2) \\
&\stackrel{(a)}{\leq} h(\underline{\boldsymbol{\theta}}_1 \mid \underline{\mathbf{x}}_1, \underline{\mathbf{y}}_1) - h(\underline{\boldsymbol{\theta}}_1 \mid \underline{\mathbf{x}}_1, \underline{\mathbf{x}}_2, \underline{\mathbf{y}}_1, \underline{\mathbf{y}}_2, \underline{\boldsymbol{\theta}}_2) \\
&\stackrel{(b)}{=} h(\underline{\boldsymbol{\theta}}_1 \mid \underline{\mathbf{x}}_1, \underline{\mathbf{y}}_1) - h(\underline{\boldsymbol{\theta}}_1 \mid \underline{\mathbf{x}}_1, \underline{\mathbf{y}}_1, \underline{\boldsymbol{\theta}}_2) \\
&= I(\underline{\boldsymbol{\theta}}_2; \underline{\boldsymbol{\theta}}_1 \mid \underline{\mathbf{x}}_1, \underline{\mathbf{y}}_1) \\
&\stackrel{(c)}{=} I(\{\boldsymbol{\theta}_{2,m}\}_0^1; \underline{\boldsymbol{\theta}}_1 \mid \underline{\mathbf{x}}_1, \underline{\mathbf{y}}_1) \\
&= h(\{\boldsymbol{\theta}_{2,m}\}_0^1 \mid \underline{\mathbf{x}}_1, \underline{\mathbf{y}}_1) - h(\{\boldsymbol{\theta}_{2,m}\}_0^1 \mid \underline{\mathbf{x}}_1, \underline{\mathbf{y}}_1, \underline{\boldsymbol{\theta}}_1) \\
&\stackrel{(d)}{=} h(\{\boldsymbol{\theta}_{2,m}\}_0^1 \mid \underline{\mathbf{x}}_1, \underline{\mathbf{y}}_1) - h(\{\boldsymbol{\theta}_{2,m}\}_0^1 \mid \underline{\boldsymbol{\theta}}_1), \tag{144}
\end{aligned}$$

where (a) holds because conditioning reduces the entropy; (b) follows since given $\underline{\boldsymbol{\theta}}_2$, $\underline{\boldsymbol{\theta}}_1$ is independent of the pair $(\underline{\mathbf{y}}_2, \underline{\mathbf{x}}_2)$; (c) follows as $\{\boldsymbol{\theta}_{2,m}\}_0^1$ is sufficient statistics for $\underline{\boldsymbol{\theta}}_2$; (d) holds since $\underline{\boldsymbol{\theta}}_2$ and $(\underline{\mathbf{y}}_1, \underline{\mathbf{x}}_1)$ are independent given $\underline{\boldsymbol{\theta}}_1$.

The first term on the RHS of (144) can be upper-bounded as

$$\begin{aligned}
h(\{\boldsymbol{\theta}_{2,m}\}_0^1 | \underline{\mathbf{x}}_1, \underline{\mathbf{y}}_1) &= h(\{\boldsymbol{\theta}_{2,m}\}_0^1 | |\underline{\mathbf{x}}_1|, \underline{\Delta}\underline{\mathbf{x}}_1, |\underline{\mathbf{y}}_1|, \underline{\Delta}\underline{\mathbf{y}}_1) \\
&= h(\{\boldsymbol{\theta}_{2,m} \stackrel{\pi}{\dashv} \underline{\Delta}\underline{\mathbf{y}}_{1,m} \stackrel{\mp}{\dashv} \underline{\Delta}\underline{\mathbf{x}}_{1,m}\}_0^1 | |\underline{\mathbf{x}}_1|, \underline{\Delta}\underline{\mathbf{x}}_1, |\underline{\mathbf{y}}_1|, \underline{\Delta}\underline{\mathbf{y}}_1) \\
&\stackrel{(a)}{\leq} h(\{\boldsymbol{\theta}_{2,m} \stackrel{\pi}{\dashv} \underline{\Delta}\underline{\mathbf{y}}_{1,m} \stackrel{\mp}{\dashv} \underline{\Delta}\underline{\mathbf{x}}_{1,m}\}_0^1 | |\underline{\mathbf{x}}_1|, \{|\underline{\mathbf{y}}_{1,m}|\}_0^1) \\
&\stackrel{(b)}{=} h(\{\boldsymbol{\theta}_{2,m} \stackrel{\pi}{\dashv} \boldsymbol{\theta}_{1,m} \stackrel{\pi}{\dashv} \underline{\Delta}(|\underline{\mathbf{x}}_{1,m}| + \mathbf{z}_{1,m})\}_0^1 | |\underline{\mathbf{x}}_1|, \{|\underline{\mathbf{y}}_{1,m}|\}_0^1) \\
&\stackrel{(c)}{=} h(\{\boldsymbol{\Delta}_2^c \stackrel{\mp}{\dashv} m\boldsymbol{\Delta}_2^r \stackrel{\pi}{\dashv} \underline{\Delta}(|\underline{\mathbf{x}}_{1,m}| + \mathbf{z}_{1,m})\}_0^1 | |\underline{\mathbf{x}}_1|, \{|\underline{\mathbf{y}}_{1,m}|\}_0^1) \\
&\stackrel{(d)}{=} h(\{\boldsymbol{\Delta}_2^c \stackrel{\mp}{\dashv} m\boldsymbol{\Delta}_2^r \stackrel{\mp}{\dashv} \underline{\Delta}(|\underline{\mathbf{x}}_{2,m}| + \mathbf{z}_{2,m})\}_0^1 | |\underline{\mathbf{x}}_2|, \{|\underline{\mathbf{y}}_{2,m}|\}_0^1) \tag{145}
\end{aligned}$$

where (a) holds because conditioning reduces entropy, (b) follows directly from (110) where $\underline{\Delta}\underline{\mathbf{y}}_{1,m} = \boldsymbol{\theta}_{1,m} \stackrel{\mp}{\dashv} \underline{\Delta}\underline{\mathbf{x}}_{1,m} \stackrel{\mp}{\dashv} \underline{\Delta}(|\underline{\mathbf{x}}_{1,m}| + \mathbf{z}_{1,m})$, and (c) holds since $\boldsymbol{\theta}_{2,m} \stackrel{\pi}{\dashv} \boldsymbol{\theta}_{1,m} = \boldsymbol{\Delta}_2^c \stackrel{\mp}{\dashv} m\boldsymbol{\Delta}_2^r$ from (5)–(6); finally, in (d) we use that $-\underline{\Delta}(|\underline{\mathbf{x}}_{1,m}| + \mathbf{z}_{1,m})$ has the same distribution as $\underline{\Delta}(|\underline{\mathbf{x}}_{2,m}| + \mathbf{z}_{2,m})$, because the phase function is symmetric and the pairs $(|\underline{\mathbf{x}}_1|, |\underline{\mathbf{x}}_2|)$ and $(\mathbf{z}_{1,m}, \mathbf{z}_{2,m})$ are exchangeable since they have the same distribution due to the i.i.d. assumption of the input distribution.

We continue with the second term on the RHS of (144)

$$\begin{aligned}
h(\{\boldsymbol{\theta}_{2,m}\}_0^1 | \underline{\boldsymbol{\theta}}_1) &\stackrel{(a)}{=} h(\boldsymbol{\theta}_2^c, \boldsymbol{\theta}_2^c \stackrel{\mp}{\dashv} \boldsymbol{\theta}_2^r | \boldsymbol{\theta}_1^c, \boldsymbol{\theta}_1^r) \\
&\stackrel{(b)}{=} h(\boldsymbol{\theta}_2^c, \boldsymbol{\theta}_2^r | \boldsymbol{\theta}_1^c, \boldsymbol{\theta}_1^r) \\
&= h(\boldsymbol{\Delta}_2^c, \boldsymbol{\Delta}_2^r), \tag{146}
\end{aligned}$$

where (a) follows since the pair $(\boldsymbol{\theta}_1^c, \boldsymbol{\theta}_1^r)$ is sufficient statistic for $\underline{\boldsymbol{\theta}}_1$ and (b) holds since the pair $(\boldsymbol{\theta}_2^c, \boldsymbol{\theta}_2^r)$ is sufficient statistics for the pair $(\boldsymbol{\theta}_2^c, \boldsymbol{\theta}_2^c \stackrel{\mp}{\dashv} \boldsymbol{\theta}_2^r)$.

Substituting (145) and (146) into (144) gives (84) and the proof is completed.

D.8 Proof of Lemma 23

By setting $\lambda = \lambda^* = (M - 1) \log e$ and $\underline{\alpha} = \underline{\alpha}^*$ in (11) we get

$$\begin{aligned}
R_{\lambda^*, \underline{\alpha}^*}(\rho, \underline{s}) &= \frac{1}{2} \mathbb{E} [\log |s_0 + \mathbf{z}_0|^2] - h(|s_0 + \mathbf{z}_0|^2 | s_0) \\
&\quad + \frac{1}{2} \mathbb{E} [\log |s_1 + \mathbf{z}_1|^2] - h(|s_1 + \mathbf{z}_1|^2 | s_1), \tag{147}
\end{aligned}$$

and employing Lemma 6 gives

$$\lim_{s_0 \rightarrow \infty} \frac{1}{2} \mathbb{E} [\log |s_0 + \mathbf{z}_0|^2] - h(|s_0 + \mathbf{z}_0|^2 | s_0) = -\frac{1}{2} \log(4\pi e), \tag{148}$$

$$\lim_{s_1 \rightarrow \infty} \frac{1}{2} \mathbb{E} [\log |s_1 + \mathbf{z}_1|^2] - h(|s_1 + \mathbf{z}_1|^2 | s_1) = -\frac{1}{2} \log(4\pi e), \tag{149}$$

which proves (86).

To characterize the asymptotic behavior of (12), we use Lemma 3 and that the phases $\underline{s}_0 + \mathbf{z}_0 \rightarrow 0$, $\underline{s}_1 + \mathbf{z}_1 \rightarrow 0$, and $\underline{s} + \mathbf{v} \rightarrow 0$ as $\underline{s} \rightarrow \infty$. Then,

$$\lim_{\underline{s} \rightarrow \infty} h\left(\left\{\Delta^c \mp m \Delta^r \mp \underline{s}_m + \mathbf{z}_m\right\}_0^1 \mid \underline{s} + \mathbf{z}\right) = h(\Delta^c, \Delta^r) \quad (150)$$

and

$$\lim_{\underline{s} \rightarrow \infty} h(\Delta^r) + h\left(\Delta^c \mp \underline{s} + \mathbf{v} \mid \|\underline{s}\| + \mathbf{v}\right) = h(\Delta^c, \Delta^r), \quad (151)$$

which results in (87) and the proof is concluded.

D.9 Proof of Lemma 24

We can start with the definition of $J(\cdot)$ from (51) and write

$$\begin{aligned} J(\alpha'_m(\gamma), \gamma) &= \alpha'_m(\gamma) + \frac{e^{-\gamma} \gamma^{\alpha'_m(\gamma)}}{\Gamma(\alpha'_m(\gamma), \gamma)} \\ &\stackrel{(a)}{\leq} \alpha'_m(\gamma) + \frac{e^{-\gamma} \gamma^{\alpha'_m(\gamma)}}{\Gamma(1, \gamma)} \\ &\stackrel{(b)}{=} \alpha'_m(\gamma) + \gamma^{\alpha'_m(\gamma)}, \end{aligned} \quad (152)$$

where (a) follows because $\Gamma(\alpha'(\gamma), \gamma) \geq \Gamma(1, \gamma)$ from Lemma 12 and (b) follows as $\Gamma(1, \gamma) = e^{-\gamma}$. Note that in (a) we could utilize Lemma 12 because $\gamma \leq x_{\max} < x_0$ and $0 \leq \alpha'(\gamma) \leq 1$.

Now, substituting (91) into (152) we can write

$$\begin{aligned} \alpha'_m(\gamma) + \gamma^{\alpha'_m(\gamma)} &= \alpha_m^* - c_m(\gamma) + \frac{\gamma^{\alpha_m^*}}{\gamma^{c_m(\gamma)}} \\ &\stackrel{(a)}{=} \alpha_m^* - c_m(\gamma) + c_m(\gamma) \\ &= \alpha_m^*, \end{aligned} \quad (153)$$

where (a) follows from (56) in Lemma 14. Thus,

$$J(\alpha'_m(\gamma), \gamma) \leq \alpha_m^*, \quad (154)$$

which proves (93).

Next we prove (94), which requires to show $\lim_{\gamma \rightarrow 0^+} c_m(\gamma) = 0$. Based on the definition of the Lambert W function we have

$$W_L(x) = \frac{x}{e^{W_L(x)}}. \quad (155)$$

Thus, we can write

$$\begin{aligned}
\lim_{\gamma \rightarrow 0^+} c_m(\gamma) &= \lim_{\gamma \rightarrow 0^+} \frac{\gamma^{\alpha_m^*} \log_e \gamma}{e^{W_L(\gamma^{\alpha_m^*} \log_e \gamma)} \log_e \gamma} \\
&= \lim_{\gamma \rightarrow 0^+} \frac{\gamma^{\alpha_m^*}}{e^{W_L(\gamma^{\alpha_m^*} \log_e \gamma)}} \\
&= \frac{0}{1} \\
&= 0,
\end{aligned} \tag{156}$$

which proves (94).

D.10 Proof of Lemma 25

In this proof, we need to characterize $g(m, \underline{s})$ for a deterministic vector

$$\underline{s} > \sqrt{\mu\gamma}. \tag{157}$$

For all $m \in \{0, \dots, M-1\}$, consider i.i.d. $\mathbf{z}_m \sim \mathcal{CN}(0, 1)$ and let

$$\varphi_m = \angle s_m + \mathbf{z}_m, \tag{158}$$

$$\begin{aligned}
\mathbf{r}_m &= |s_m + \mathbf{z}_m| \\
&= s_m (1 + O(1/\sqrt{\mu\gamma})).
\end{aligned} \tag{159}$$

Then, according to Lemma 9, given s_m and $\mathbf{r}_m = r_m$, we have $\varphi_m \sim \mathcal{VM}(0, 2s_m r_m)$ with its pdf denoted by $f_{\varphi_m}^{\text{VM}}(\varphi_m; 0, 2s_m r_m)$. Using Lemma 10, the pdf of a von Mises distribution can be approximated by a wrapped normal distribution as

$$f_{\varphi_m}^{\text{VM}}(\varphi_m; 0, 2s_m r_m) \stackrel{(a)}{=} f_{\varphi_m}^{\text{WN}}\left(\varphi_m; 0, \frac{1}{2s_m r_m}\right) + O\left(\frac{1}{\sqrt{s_m r_m}}\right). \tag{160}$$

We need to evaluate the two terms on the RHS of (14), which can be reformulated as

$$h(\angle s_m + \mathbf{z}_m \mid s_m, |s_m + \mathbf{z}_m|) = h(\varphi_m \mid s_m, \mathbf{r}_m), \tag{161}$$

$$h(\phi(m, \underline{s}) \mid \underline{s}, \{|s_i + \mathbf{z}_i|\}_{i=0}^m) = h(\phi(m, \underline{s}) \mid \underline{s}, \{\mathbf{r}_i\}_{i=0}^m). \tag{162}$$

To evaluate the RHS of (161), we use Lemma 15 and write

$$\begin{aligned}
h(\varphi_m \mid s_m, \mathbf{r}_m) &= \frac{1}{2} \log(2\pi e) - \frac{1}{2} \log(2s_m r_m) + O\left(\frac{1}{\sqrt{s_m r_m}}\right) \\
&\stackrel{(a)}{=} \frac{1}{2} \log(2\pi e) - \frac{1}{2} \log(2s_m^2) + O\left(\frac{1}{\sqrt{\mu\gamma}}\right),
\end{aligned} \tag{163}$$

where (a) follows from (159).

To evaluate the RHS of (162), we approximate each term of $\phi(m, \underline{s})$ in (15) with a wrapped normal random variable. Thus, for given m and \underline{s} , the conditional distribution of $\phi(m, \underline{s})$ can be approximated by a summation of wrapped normal random variables

$$f_{\phi(m, \underline{s})}(\varphi) = f_{\phi(m, \underline{s})}^{\text{WN}}(\varphi; 0, a(m, \underline{s})) + O(a(m, \underline{s})), \quad (164)$$

where

$$\begin{aligned} a(m, \underline{s}) &= \begin{cases} \frac{1}{2s_2r_2} + \frac{2}{s_1r_1} + \frac{1}{2s_0r_0}, & m = 2, \\ \sum_{i=m-3}^m \frac{1}{2s_i r_i}, & m > 2, \end{cases} \\ &= \begin{cases} \frac{1}{2s_2^2} + \frac{2}{s_1^2} + \frac{1}{2s_0^2} + O\left(\frac{1}{\sqrt{\mu\gamma}}\right), & m = 2, \\ \sum_{i=m-3}^m \frac{1}{2s_i^2} + O\left(\frac{1}{\sqrt{\mu\gamma}}\right), & m > 2. \end{cases} \end{aligned} \quad (165)$$

Using Lemma 15 and (165), we can write

$$\begin{aligned} h(\phi(m, \underline{s}) \mid \underline{s}, \{\mathbf{r}_i\}_{i=0}^m) &= \frac{1}{2} \log(2\pi e) + \frac{1}{2} \log(a(m, \underline{s})) + O\left(\sqrt{a(m, \underline{s})}\right) \\ &= \frac{1}{2} \log(2\pi e) + \begin{cases} \frac{1}{2} \log\left(\frac{1}{2s_2^2} + \frac{2}{s_1^2} + \frac{1}{2s_0^2}\right) + O\left(\frac{1}{\sqrt{\mu\gamma}}\right), & m = 2, \\ \frac{1}{2} \log\left(\sum_{i=m-3}^m \frac{1}{2s_i^2}\right) + O\left(\frac{1}{\sqrt{\mu\gamma}}\right), & m > 2. \end{cases} \end{aligned} \quad (166)$$

Finally, substituting (163) and (166) into (161) and (162), respectively; then, (161) and (162) into (14) gives (103), and the proof is completed.

REFERENCES

- [1] G. Colavolpe, "Communications over phase-noise channels: A tutorial review," in *6th Advanced Satellite Multimedia Systems Conference (ASMS) and 12th Signal Processing for Space Communications Workshop (SPSC)*, 2012, pp. 316–327.
- [2] A. Lapidoth, "On phase noise channels at high SNR," in *Proc. IEEE Information Theory Workshop (ITW)*, 2002.
- [3] M. Katz and S. Shamai, "On the capacity-achieving distribution of the discrete-time noncoherent and partially coherent AWGN channels," *IEEE Transactions on Information Theory*, vol. 50, no. 10, pp. 2257–2270, 2004.
- [4] L. Barletta, M. Magarini, and A. Spalvieri, "The information rate transferred through the discrete-time Wiener's phase noise channel," *Journal of Lightwave Technology*, vol. 30, no. 10, pp. 1480–1486, 2012.
- [5] L. Barletta and G. Kramer, "Upper bound on the capacity of discrete-time Wiener phase noise channels," in *Proc. IEEE Information Theory Workshop (ITW)*, 2015.
- [6] M. R. Khanzadi, R. Krishnan, J. Söder, and T. Eriksson, "On the capacity of the Wiener phase-noise channel: Bounds and capacity-achieving distributions," *IEEE Transactions on Communications*, vol. 63, no. 11, pp. 4174–4184, 2015.
- [7] H. Ghozlan and G. Kramer, "Models and information rates for Wiener phase noise channels," *IEEE Transactions on Information Theory*, vol. 63, no. 4, pp. 2376–2393, 2017.
- [8] G. Durisi, A. Tarable, C. Camarda, and G. Montorsi, "On the capacity of MIMO Wiener phase-noise channels," in *Proc. Information Theory and Applications Workshop (ITA)*, 2013.
- [9] G. Durisi, A. Tarable, C. Camarda, R. Devassy, and G. Montorsi, "Capacity bounds for MIMO microwave backhaul links affected by phase noise," *IEEE Transactions on Communications*, vol. 62, no. 3, pp. 920–929, 2014.

- [10] M. R. Khanzadi, G. Durisi, and T. Eriksson, "Capacity of SIMO and MISO phase-noise channels with common/separate oscillators," *IEEE Transactions on Communications*, vol. 63, no. 9, pp. 3218–3231, 2015.
- [11] S. Yang and S. Shamai, "On the multiplexing gain of discrete-time MIMO phase noise channels," *IEEE Transactions on Information Theory*, vol. 63, no. 4, pp. 2394–2408, 2017.
- [12] A. Ishizawa, T. Nishikawa, A. Mizutori, H. Takara, A. Takada, T. Sogawa, and M. Koga, "Phase-noise characteristics of a 25-GHz-spaced optical frequency comb based on a phase-and intensity-modulated laser," *Optics express*, vol. 21, no. 24, pp. 29 186–29 194, 2013.
- [13] V. Ataie, E. Temprana, L. Liu, E. Myslivets, B. P.-P. Kuo, N. Alic, and S. Radic, "Ultrahigh count coherent WDM channels transmission using optical parametric comb-based frequency synthesizer," *Journal of Lightwave Technology*, vol. 33, no. 3, pp. 694–699, 2015.
- [14] M. Mazur, A. Lorences-Riesgo, J. Schröder, P. A. Andrekson, and M. Karlsson, "High spectral efficiency PM-128QAM comb-based superchannel transmission enabled by a single shared optical pilot tone," *Journal of Lightwave Technology*, vol. 36, no. 6, pp. 1318–1325, 2018.
- [15] L. Lundberg, M. Karlsson, A. Lorences-Riesgo, M. Mazur, V. Torres-Company, J. Schröder, and P. A. Andrekson, "Frequency comb-based WDM transmission systems enabling joint signal processing," *Applied Sciences*, vol. 8, no. 5, pp. 718, 2018.
- [16] L. Lundberg, M. Mazur, A. Fülöp, V. Torres-Company, M. Karlsson, and P. A. Andrekson, "Phase correlation between lines of electro-optical frequency combs," in *Proc. Conference on Lasers and Electro-Optics (CLEO)*, JW2A.149, 2018.
- [17] A. Lapidoth and S. M. Moser, "Capacity bounds via duality with applications to multiple-antenna systems on flat-fading channels," *IEEE Transactions on Information Theory*, vol. 49, no. 10, pp. 2426–2467, 2003.
- [18] L. Lundberg, M. Mazur, A. Mirani, B. Foo, J. Schröder, V. Torres-Company, M. Karlsson, and P. A. Andrekson, "Phase-coherent lightwave communications with frequency combs," *Nature Communications*, vol. 11, no. 1, pp. 201–212, 2020.
- [19] A. J. Metcalf, V. Torres-Company, D. E. Leaird, and A. M. Weiner, "High-power broadly tunable electrooptic frequency comb generator," *IEEE Journal of Selected Topics in Quantum Electronics*, vol. 19, no. 6, pp. 231–236, 2013.
- [20] L. Lundberg, M. Mazur, A. Lorences-Riesgo, M. Karlsson, and P. A. Andrekson, "Joint carrier recovery for DSP complexity reduction in frequency comb-based superchannel transceivers," in *Proc. European Conference on Optical Communication (ECOC)*, 2017.
- [21] M. Farsi, M. Karlsson, and E. Agrell, "Pilot distributions for phase noise estimation in electro-optic frequency comb systems," in *Proc. European Conference on Optical Communication (ECOC)*, 2023, paper We.A.7.1.
- [22] J. A. Nelder and R. Mead, "A simplex method for function minimization," *The Computer Journal*, vol. 7, no. 4, pp. 308–313, 1965.
- [23] Z. Szabó, "Information theoretical estimators toolbox," *The Journal of Machine Learning Research*, vol. 15, no. 1, pp. 283–287, 2014.
- [24] F. Lei, Z. Ye, Ó. B. Helgason, A. Fülöp, M. Girardi, and V. Torres-Company, "Optical linewidth of soliton microcombs," *Nature Communications*, vol. 13, no. 1, pp. 3161–3170, 2022.
- [25] S. M. Moser, "The fading number of multiple-input multiple-output fading channels with memory," *IEEE Transactions on Information Theory*, vol. 55, no. 6, pp. 2716–2755, 2009.
- [26] H. Fu and P. Y. Kam, "Exact phase noise model and its application to linear minimum variance estimation of frequency and phase of a noisy sinusoid," in *Proc. IEEE International Symposium on Personal, Indoor and Mobile Radio Communications (PIMRC)*, 2008.

- [27] J. Kent, "Limiting behaviour of the von Mises-Fisher distribution," in *Mathematical Proceedings of the Cambridge Philosophical Society*, vol. 84, no. 3. Cambridge University Press, 1978, pp. 531–536.
- [28] K. V. Mardia, P. E. Jupp, and K. Mardia, *Directional Statistics*. Wiley Online Library, 2000, vol. 2.
- [29] F. W. J. Olver, D. W. Lozier, R. F. Boisvert, and C. W. Clark, *NIST Handbook of Mathematical Functions*. Cambridge University Press, 2010.
- [30] R. M. Corless, G. H. Gonnet, D. E. Hare, D. J. Jeffrey, and D. E. Knuth, "On the Lambert W function," *Advances in Computational Mathematics*, vol. 5, pp. 329–359, 1996.
- [31] J. V. Michalowicz, J. M. Nichols, and F. Bucholtz, *Handbook of Differential Entropy*. Chapman & Hall/CRC, 2013.